

**The FNR-type regulator GoxR of the obligatory aerobic acetic acid bacterium
Gluconobacter oxydans affects expression of genes involved in respiration and redox
metabolism**

Stefanie Schweikert^{a*#}, Angela Kranz^{a#}, Toshiharu Yakushi^b, Andrei Filipchuk^a, Tino Polen^a,
Helga Etterich^a, Stephanie Bringer^a, and Michael Bott^{#a}

^aIBG-1: Biotechnology, Institute of Bio- and Geosciences, Forschungszentrum Jülich,
D-52425 Jülich, Germany

^bDepartment of Biological Chemistry, Faculty of Agriculture, Yamaguchi University, Yamaguchi
753-8515, Japan

Running title: The FNR-type regulator GoxR of *Gluconobacter oxydans*

Keywords: *Gluconobacter oxydans*, transcriptional regulator, FNR, oxygen limitation,
transhydrogenase, ethanol

[#]Address correspondence to Michael Bott, m.bott@fz-juelich.de
<https://orcid.org/0000-0002-4701-8254>

[#]These authors contributed equally to this work. Author names are in order of increasing
seniority.

*Present address: Dr. Stefanie Schweikert, Sanofi-Aventis Deutschland GmbH, Industriepark
Höchst, 65926 Frankfurt am Main, Germany

24

25

ABSTRACT

Gene expression in the obligately aerobic acetic acid bacterium *Gluconobacter oxydans* responds to oxygen limitation, but the regulators involved are unknown. In this study, we analyzed a transcriptional regulator named GoxR (GOX0974), which is the only member of the FNR family in this species. Evidence was obtained that GoxR contains an iron-sulfur cluster, suggesting that GoxR functions as an oxygen sensor similar to FNR. The direct target genes of GoxR were determined by combining several approaches including a transcriptome comparison of a Δ *goxR* mutant with the wild type and detection of *in vivo* GoxR binding sites by ChAP-Seq. Prominent targets were the *cioAB* genes encoding a cytochrome *bd* oxidase with low O₂ affinity, which were repressed by GoxR, and the *pnt* operon, which was activated by GoxR. The *pnt* operon encodes a transhydrogenase (*pntA1A2B*), an NADH-dependent oxidoreductase (GOX0313), and another oxidoreductase (GOX0314). Evidence was obtained for GoxR being active despite a high dissolved oxygen concentration in the medium. We suggest a model in which the very high respiration rates of *G. oxydans* due to the periplasmic oxidations cause an oxygen-limited cytoplasm and insufficient reoxidation of NAD(P)H in the respiratory chain, leading to an inhibited cytoplasmic carbohydrate degradation. GoxR-triggered induction of the *pnt* operon enhances fast interconversion of NADPH and NADH by the transhydrogenase and NADH reoxidation by the GOX0313 oxidoreductase *via* reduction of acetaldehyde formed by pyruvate decarboxylase to ethanol. In fact, small amounts of ethanol were formed by *G. oxydans* under oxygen-restricted conditions in a GoxR-dependent manner.

IMPORTANCE

Gluconobacter oxydans serves as cell factory for oxidative biotransformations based on membrane-bound dehydrogenases and as model organism for elucidating the metabolism of acetic acid bacteria. Surprisingly, to our knowledge none of the more than 100 transcriptional regulators encoded in the genome of *G. oxydans* has been studied experimentally up to now. In this work, we analyzed the function of a regulator named GoxR, which belongs to the FNR family. Members of this family serve as oxygen sensors by means of an oxygen-sensitive [4Fe-4S] cluster and typically regulate genes important for growth under anoxic conditions by anaerobic respiration or fermentation. Because *G. oxydans* has an obligatory aerobic respiratory mode of energy metabolism, it was tempting to elucidate the target genes regulated by GoxR. Our results show that GoxR affects the expression of genes that support the interconversion of NADPH and NADH and NADH reoxidation by reduction of acetaldehyde to ethanol.

INTRODUCTION

Gluconobacter oxydans is a Gram-negative, rod-shaped α -proteobacterium belonging to the family of acetic acid bacteria (1). It has been used since the 1930s in biotechnology, mainly in production of vitamin C and 6-amino-L-sorbose, a key intermediate for the synthesis of the anti-diabetic drug miglitol (2-4). The basis for its industrial application is the variety of membrane-bound dehydrogenases, which incompletely oxidize sugars, sugar alcohols, and a variety of other compounds regio- and stereoselectively in the periplasm, such as D-sorbitol to L-sorbose in vitamin C synthesis (5-7). The membrane-bound dehydrogenases use ubiquinone as electron acceptor, which is reoxidized either by the proton-pumping cytochrome *bo*₃-type oxidase (8) or by a cytochrome *bd*-type oxidase (9). The latter enzyme was characterized as cyanide-insensitive

oxidase CIO and the corresponding genes named *cioA* and *cioB* instead of *cydA* and *cydB* (10, 11). Remarkably, the oxygen affinity of CIO was found to be 7-fold lower than that of cytochrome *bo₃* (21 μ M vs. 3 μ M), which is in contrast to the situation in *Escherichia coli*, where cytochrome *bd* is a high-affinity terminal oxidase (11, 12).

When *G. oxydans* is cultivated with substrates such as glucose or mannitol, about 90% of these carbon sources are converted by membrane-bound dehydrogenases to partially oxidized products, which remain unmetabolized in the medium. Only a small fraction of the substrate or its oxidation products enter the cell and are metabolized either in the pentose phosphate pathway (PPP) or the Entner-Doudoroff pathway (EDP). The PPP, which runs partially cyclically, is the major catabolic pathway for glucose in the cytoplasm as shown by ¹³C-metabolic flux analysis and studies of mutants lacking key enzymes of the PPP or the EDP (13-15). Neither glycolysis nor the tricarboxylic acid (TCA) cycle is functional, since *G. oxydans* lacks the genes for phosphofructokinase, succinyl-CoA synthetase, and succinate dehydrogenase (16, 17). The absence of a functional TCA cycle explains the inability of *G. oxydans* to oxidize acetate, which is a key difference to other acetic acid bacteria, such as *Acetobacter* and *Gluconacetobacter* species. Pyruvate formed by the PPP or the EDP is predominantly converted to acetate via the activities of pyruvate decarboxylase and an NADP⁺-dependent acetaldehyde dehydrogenase (18). Metabolic engineering of *G. oxydans* including the inactivation of glucose oxidation to gluconate and of pyruvate decarboxylation combined with the introduction of the missing TCA cycle genes led to strains with increased biomass yield on glucose that form pyruvate instead of acetate (17, 19).

According to the genome sequence and current literature, *G. oxydans* 621H is not capable of anaerobic growth by respiratory or fermentative pathways and is, therefore, described as a strictly aerobic bacterium (16, 20). However, it responds to changes in the oxygen concentration, because

a shift from oxygen excess to oxygen limitation caused expression changes of about 500 genes, many of which are involved in respiration and oxidative phosphorylation (21). Although the expression changes of many genes of the oxygen starvation stimulon might have been triggered by the slowed, non-exponential growth occurring after the shift to oxygen limitation, oxygen- or redox-sensing transcriptional regulators might also be involved. In bacteria, several types of oxygen sensors have been described, e.g. those based on iron-sulfur clusters, exemplified by FNR-type transcriptional regulators, and those based on heme, exemplified by the FixL sensor kinase (for reviews see (22-30)).

In this study, we characterized a transcriptional regulator of the FNR family in *G. oxydans*, which we named *Gluconobacter redox* regulator, GoxR (GOX0974). Based on the determined target genes of GoxR we propose a model for the response of *G. oxydans* to oxygen limitation.

RESULTS

***In silico* analysis of GoxR suggests an FNR-like function.**

Inspection of the genome of *G. oxydans* (16, 20) for transcriptional regulators that might be involved in oxygen-dependent gene expression revealed a gene (GOX0974, termed *goxR*) encoding a protein (26.5 kDa, 240 amino acid residues) which belongs to the Crp/FNR family of transcriptional regulators. GoxR is the only member of this family present in *G. oxydans*. The Crp/FNR family includes various subfamilies represented by the cAMP receptor protein Crp, the fumarate-nitrate-reduction regulator FNR, or the FixK regulator involved in nitrogen fixation (25). A search using the NCBI BlastP tool (31) revealed proteins with an e-value of $<2e^{-63}$ and $>50\%$ sequence identity to GoxR in species of the genera *Gluconobacter*, *Saccharibacter*, *Kozakia*, *Asaia*, *Acidomonas*, *Gluconacetobacter*, *Komagataeibacter*, and *Acetobacter*, all of which belong to the

family *Acetobacteraceae*. A comparison of GoxR with the *E. coli* proteome revealed FNR as the closest homolog with 30% amino acid sequence identity, whereas the cAMP-binding regulator Crp showed only 22% sequence identity with GoxR. The strongest evidence for GoxR being a member of the FNR subfamily was provided by the presence of five cysteine residues in the N-terminal region: C₁₄(X)₂C₁₇(X)₇C₂₅(X)₅C₃₁(X)₈₂C₁₁₃ (Fig. S1). The presence of four cysteine residues is characteristic for FNR-like proteins, because they are required for the formation of the [4Fe-4S] cluster that is key for FNR function, and these residues are not present in members of the Crp subfamily. In *E. coli* FNR, the residues C₂₀, C₂₃, C₂₉, and C₁₂₂ are known to coordinate the [4Fe-4S] cluster, whereas C₁₆ has been reported to serve as a stabilizing residue (32).

Comparison of global gene expression in the Δ goxR mutant and the parental strain by RNA-Seq.

To explore the function of GoxR, a mutant with an in-frame deletion of *goxR* was constructed in the parental strain *G. oxydans* Δ hsdR. The *hsdR* gene (GOX2567) is part of a restriction-modification system located on the 163 kb plasmid pGOX1 and was deleted in order to improve transformation efficiency. Growth of *G. oxydans* Δ goxR in mannitol medium was comparable to the parental strain both in shake flasks and in bioreactors under oxygen- and pH-controlled conditions (15% dissolved oxygen (DO), pH 6) (data not shown). A transcriptome comparison of the Δ goxR mutant and the parental strain was performed by RNA-Seq to identify genes with altered expression in the absence of GoxR. For this purpose, the two strains were cultivated in a bioreactor at 15% DO and pH 6 using mannitol medium. Because GoxR was assumed to be active under oxygen-restricted conditions, the oxygen supply was switched from 15% DO to 0% DO by gassing

with a mixture of 2% O₂/98% N₂ when the strains had reached an OD₆₀₀ of 2.5. The cells were harvested 20 min after the switch and used for RNA isolation.

In three independent biological replicates, two genes showed a ≥ 2 -fold increased mRNA level in the $\Delta goxR$ mutant and 12 genes a ≥ 2 -fold decreased mRNA level with p-values ≤ 0.05 (Table 1). The genes with an increased expression in the $\Delta goxR$ mutant were *cioAB* encoding the two subunits of the *bd*-type terminal oxidase CIO (see Introduction). Within the group of genes with a decreased expression in the $\Delta goxR$ mutant, the ones showing the most strongly reduced mRNA levels were those of the *pnt* operon: *pntA1-pntA2-pntB*-GOX0313-GOX0314 (Fig. 1). The first three genes of this operon encode the subunits $\alpha 1$, $\alpha 2$, and β of a membrane-bound transhydrogenase, which catalyzes the reversible reduction of NADP⁺ with NADH coupled to the import of a proton from the periplasm to the cytoplasm (33). GOX0313 encodes a medium-chain alcohol dehydrogenase with a broad substrate spectrum that oxidizes various primary alcohols, but has a preference for NADH-dependent reduction of aldehydes to alcohols and of α -diketones to (*S*)-hydroxyketones (34). GOX0314 was annotated as an alcohol dehydrogenase-like oxidoreductase, but it has not yet been experimentally characterized. A group of six genes involved in flagella synthesis organized in several operons showed an approximately 3-fold reduced mRNA level in the $\Delta goxR$ mutant, suggesting an influence of GoxR on motility. Another gene with a 2.5-fold reduced mRNA level in the $\Delta goxR$ mutant was GOX0090, originally annotated as putative sugar kinase. However, the GOX0090 protein shows 30% sequence identity to the YjeF protein of *Escherichia coli*, which has been shown to function as an enzymatic repair system for hydrated NAD(P)H (35) and a similar function can be assumed for the *G. oxydans* homolog.

Reporter gene assays for potential GoxR target genes.

In order to confirm the RNA-Seq results, reporter gene assays were performed with three potential GoxR target genes, *cioA*, *pntA1*, and GOX0090. The DNA regions covering 314 – 340 bp upstream of the predicted start codon of the three genes were cloned into the promoter probe vector pLacZ_pPPP3 carrying a *lacZ* reporter gene. The resulting plasmids pLacZ_*cioA*, pLacZ_*pntA1*, and pLacZ_0090 as well as the promoter-less *lacZ* control plasmid (pLacZ), were transferred into the *G. oxydans* parent and Δ *goxR* strains by electroporation. The strains were cultivated in a bioreactor in the same way as the strains used for the RNA-Seq analysis and used 0, 20, and 60 min after the shift from 15% DO to 0% DO (by gassing with a mixture of 2% O₂/98% N₂) for β -galactosidase assays.

As shown in Fig. 2, the background LacZ activity in the two control strains carrying pLacZ_control varied between 61 and 114 Miller units. The parental strain carrying pLacZ_*cioA* showed LacZ activities around 30 Miller units that were even lower than with pLacZ_control at all time points tested. This suggests that *cioA* expression is very low under the chosen conditions and that in the plasmid pLacZ_control there is some residual *lacZ* expression from a plasmid-based promoter. In the Δ *goxR* mutant carrying pLacZ-*cioA*, the LacZ activity was 31-fold higher than in the parental strain already at high oxygen levels and 45-fold or 59-fold higher 20 min and 60 min after the shift to oxygen limitation. These results suggest that GoxR inhibits *cioA* expression. The parental strain carrying pLacZ_*pntA1* showed very high LacZ activities (4486 Miller units) already at 15% DO, which further increased about 1.5-fold after the shift to oxygen limitation. In the Δ *goxR* mutant with pLacZ_*pntA1*, the LacZ activity (959 Miller units) was 4.7-fold lower than in the parental strain at 15% DO, but also increased about 2-fold after the shift to oxygen limitation. These results suggest that GoxR stimulates expression of the *pnt* operon and that an additional regulator or regulatory mechanism is responsible for increased expression after the shift to oxygen limitation.

The LacZ activity for pLacZ_0090 in the parental strain was 15-fold lower than for *pntAI* and increased 2.6-fold after the switch to oxygen limitation. In the $\Delta goxR$ mutant with pLacZ_0090, the LacZ activities were at background level, suggesting that GoxR stimulates GOX0090 expression.

The results from the reporter gene studies are in agreement with the RNA-Seq data. The observation that the LacZ activities of the $\Delta goxR$ mutant and the parental strain differed already before the switch to oxygen limitation for all three tested genes suggests that GoxR is active in the parental strain already at 15% DO.

Aldehyde reductase activity of the soluble cell fraction

As another approach to confirm the influence of GoxR on the expression of the *pnt* operon, we measured NADH-dependent reduction of propionaldehyde and hydrocinnamaldehyde in the soluble cell fraction of the parental strain and the $\Delta goxR$ mutant. These substances were previously identified as favorable substrates for the purified GOX0313 oxidoreductase (34). In the parental strain, the activities for both substrates increased 1.5- to 2-fold after the shift from 15% DO to 0% DO (Fig. 3). In the $\Delta goxR$ mutant, both activities were much lower (7- to 15-fold) than in the parental strain and did not change much after the shift from 15% DO to 0% DO (Fig. 3). These results are in agreement with the assumption that both reductase activities are predominantly catalyzed by GOX0313, whose expression was found to be 7-fold decreased in the $\Delta goxR$ mutant (Table 1). Furthermore, in agreement with the reporter gene studies, the enzyme activity differences between the $\Delta goxR$ mutant and the parental strain were already present under oxygen-saturating conditions, supporting the assumption that GoxR is active at a DO level of 15%.

Ethanol formation by *G. oxydans* under oxygen-restricted conditions.

We previously speculated that GOX0313 activity might play a role in the adjustment of the redox balance of NAD⁺ and NADH under oxygen-limited conditions because expression of the GOX0313 gene was upregulated under oxygen limitation together with the other genes of the *pnt* operon (21). Of the various substrates identified for GOX0313 (34), acetaldehyde was reduced with the highest specific activity and is also a likely *in vivo* substrate, as cytoplasmic carbon catabolism involves decarboxylation of pyruvate to acetaldehyde (18, 19). Under conditions of a high NADH/NAD⁺ ratio caused by oxygen limitation or insufficient NADH dehydrogenase activity, acetaldehyde may serve as the electron acceptor for NADH reoxidation by an alcohol dehydrogenase, forming ethanol as product. Therefore, we examined ethanol production by cell suspensions of the parental strain and of the Δ *goxR* mutant incubated under oxygen-restricted conditions in a buffer containing glucose. As shown in Fig. 4, the parental strain indeed produced some ethanol in a time-dependent manner. The Δ *goxR* mutant also formed ethanol, but at a much lower rate than the parental strain, correlating with a lower expression of the GOX0313 oxidoreductase.

Identification of a putative DNA-binding motif of GoxR.

Because the amino acid sequence of the DNA-recognition helix of the helix-turn-helix motif of GoxR (ETVSR) is almost identical to the one of *E. coli* FNR (ETISR, Fig. S1), we assumed that the DNA-binding site of GoxR is similar to the one of FNR. The consensus sequence reported for FNR-binding sites in *E. coli* is TTGAT-N₄-ATCAA (25, 36). We therefore analyzed the promoter regions (500 bp upstream of start codon plus 50 bp coding region) of selected genes or operons with altered expression in the Δ *goxR* mutant for the presence of sequence motifs with similarity to

the *E. coli* FNR consensus motif using the FIMO program (37) of the MEME bioinformatics suite (38).

In the case of *cioA*, a potential GoxR binding site (**TTGATttttGTCAA**) was centered at position -56.5 upstream of the transcriptional start site (TSS, 128 bp upstream of the annotated ATG start codon), which was identified by 5'-RACE (Fig. S2) and by reanalysis of RNA-Seq mapping data (39). Another less conserved potential GoxR binding site (**TTTAGagggTTCAA**) was centered at position -2.5 with respect to the TSS, which would be compatible with *cioAB* repression by GoxR (Fig. S3). In a previous RNA-Seq analysis, a potential TSS was identified within the coding region of *cioA* and another potential TSS was located in the 3'-region of the upstream gene GOX0277 (39). The relevance of these potential TSSs is unclear.

In the case of the *pnt* operon, a sequence perfectly matching the FNR consensus sequence (**TTGATatccATCAA**) was centered at position -41.5 with respect to the TSS (Fig. S3), which was located 80 bp upstream of the annotated start codon by RNA-Seq (39) and confirmed in this work by 5'-RACE (Fig. S2). For the GOX0090 gene, a putative GoxR-binding site (**TTGATcctcGTCAT**) was also located at position -41.5 with respect to the TSS (Fig. S3) identified by RNA-Seq 132 bp upstream of the start codon (39). However, this TSS was not detected by the automatic pipeline, but also by re-checking of the respective mapping. Position -41.5 matches with class II FNR-activated promoters (40) and supports an activating function of GoxR for the *pnt* operon and GOX0090.

Genome-wide identification of *in vivo* GoxR-binding sites by ChAP-Seq analysis

In order to demonstrate that the GoxR sequence motifs identified by bioinformatic means are indeed bound by GoxR *in vivo* and to identify further GoxR binding sites, we performed a ChAP-

255 Seq experiment using a *G. oxydans* strain in which the chromosomal *goxR* gene was modified by
256 a 3'-terminal extension resulting in a GoxR variant with a C-terminal Streptag preceded by a short
257 linker (SAWSHPQFEK). The strain was cultivated in a 5-l baffled Erlenmeyer flask with 1 l
258 medium at 130 rpm and cells were harvested at an OD₆₀₀ of about 2.8 and used for isolation of
259 GoxR-bound DNA (see Materials and Methods). 43 GoxR binding sites were identified in the
260 genome of *G. oxydans*, 34 of which were located upstream of open reading frames (ORFs) (Table
261 S1). A search for the presence of the *E. coli* FNR consensus motif (TTGAT-N₄-ATCC) in a 100-
262 bp DNA region comprising 50 bp each upstream and downstream of the peak maximum revealed
263 9 ChAP-Seq peaks that contained two binding motifs and 8 ChAP-Seq peaks with a single binding
264 motif (Table S1). For 17 ChAP-Seq peaks, no binding motif was identified.

265 With the exception of six genes involved in flagella synthesis, *in vivo* GoxR binding was found
266 upstream of all genes and operons that were shown to have a ≥ 2 -fold altered mRNA level in the
267 RNA-Seq analysis, which are the *pnt* operon, the *cioAB* operon, and GOX0090. In Fig. 5, the
268 ChAP-Seq plots of the corresponding peaks, the identified binding site motifs, and the mRNA
269 ratios ($\Delta goxR$ vs. parental strain) are shown. In all three cases, the binding motifs identified by
270 bioinformatic means were present in the peak regions. In addition to the GoxR targets described
271 above, ChAP-Seq identified GoxR binding sites upstream of five genes with a ≥ 2 -fold altered
272 mRNA level in the $\Delta goxR$ mutant, which were not included in Table 1, because the mRNA ratios
273 did not meet the p-value ≤ 0.05 criterion (Fig. 5, Table S1). Four of these genes showed an increased
274 expression in the $\Delta goxR$ mutant, which are *trxA* encoding thioredoxin (mRNA ratio 3.06, p-value
275 0.10), *hemH* coding for a ferroxidase (mRNA ratio 2.21, p-value 0.22), and the GOX1500-
276 GOX1501 operon coding for a putative toxin-antitoxin system (mRNA ratios 2.28 and 2.04, p-
277 values 0.18 and 0.22). The GoxR binding sites were centered at positions +37.5, +94.5, and +13.5

with respect to the TSSs of *trxA*, *hemH*, and GOX1500, respectively, supporting a repressor function of GoxR for these genes. In the case of GOX2142 encoding a hypothetical protein, expression was decreased in the $\Delta goxR$ mutant (mRNA ratio 0.46, p-value: 0.06) and the GoxR binding motif was located at position -41.5 with respect to the TSS (39), suggesting that expression of GOX2142 is activated by GoxR.

Several genes that were found by ChAP-Seq to contain a GoxR binding site in the promoter region did not show an altered expression in the $\Delta goxR$ mutant, such as GOX1988 (pyridoxine/pyridoxamine 5'-phosphate oxidase), GOX1070 (transcription termination factor Rho), GOX0691 (hemolysin D), GOX0692 (TetR family transcriptional regulator), GOX0875 (bacterial archaeo-eukaryotic release factor family 12), GOX0091 (hypothetical protein), or GOX0978 (riboflavin biosynthesis protein RibD) (Table S1). Therefore, the role of GoxR for expression of these genes remains unclear.

Evidence for the presence of an iron-sulfur cluster in GoxR.

For biochemical characterization of GoxR, the expression plasmid pMal-c-*goxR* was constructed, which encodes a 69.6 kDa fusion protein composed of the *E. coli* maltose-binding protein (MBP) without its signal peptide followed by a TEV cleavage site and the GoxR sequence. The fusion with MBP allowed overproduction of GoxR as a soluble protein in *E. coli* BL21(DE3), whereas overproduction of another GoxR variant with an N-terminal decahistidine tag followed by a TEV cleavage site using plasmid pET-TEV-*goxR* led to the formation of inclusion bodies (data not shown). In initial cultivation and purification experiments that were performed under aerobic conditions, an induction with 0.5 mM IPTG at an OD₆₀₀ of 0.5 to 0.8 followed by cultivation overnight at 16 °C was selected as suitable conditions for overproduction. For the purification of

MBP-GoxR with amylose resin, the conditions suggested by the manufacturer (New England Biolabs) were applied. The anaerobic purification of MBP-GoxR was performed in an anaerobic chamber as described in Materials and Methods. The cell-free extract already had a dark green to brownish color, which was recovered in the elution fractions 3 to 6, suggesting the presence of an iron-sulfur cluster in the purified protein (Fig. S4). The fractions were analyzed by SDS-PAGE and found to contain a protein of the expected mass of ~69 kDa (data not shown). A UV/VIS spectrum of elution fraction 3 of the anaerobically purified GoxR revealed besides the 280 nm peak a small peak at 420 nm, which suggested the presence of an iron-sulfur cluster (Fig. S4). After aerobic incubation of the same sample for 7 h, the brownish to dark green color disappeared and also the 420 nm peak of the spectrum, suggesting the destruction of an oxygen-labile iron-sulfur cluster (Fig. S4).

Identification of cysteine residues required for GoxR activity.

In order to identify the cysteine residues that are involved in the formation of the iron-sulfur cluster, GoxR variants were constructed in which each of the five N-terminal cysteine residues C14, C17, C25, C31, and C113 was exchanged individually to alanine using pTrc99a-*goxR* as parental expression plasmid. The activity of the five GoxR variants was tested in an *E. coli* Δ *fnr* strain which contained the *goxR* expression plasmids and the reporter plasmid pLacZ-*cioA*. As controls, pTrc99a and pLacZ were used. *E. coli* was used for this experiment as currently no compatible plasmid vectors are available for *G. oxydans*. As reported above, *cioA* expression is assumed to be repressed by GoxR and inactive GoxR variants should lead to increased expression of *lacZ* under control of the *cioA* promoter. After anaerobic cultivation, the LacZ activity of the various strains was measured and the values determined in the absence of GoxR was set as 100%

(Fig. 6). In the presence of wild-type GoxR, LacZ activity was reduced by 70%, suggesting that GoxR synthesized in *E. coli* is functional and able to repress the *cioA* promoter. In contrast to wild-type GoxR, the variants GoxR-C17A, GoxR-C25A, and GoxR-C113A showed the same LacZ activity as the control without GoxR, suggesting that residues C17, C25, and C113 are essential for the synthesis of a repression-competent GoxR protein and therefore presumably involved in formation of the Fe-S cluster. The variant GoxR-C14A showed an intermediate LacZ activity, corresponding to about 50% of the value found in the absence of GoxR, suggesting that also C14 is important for GoxR-dependent repression and presumably involved in Fe-S cluster formation. The variant GoxR-C31A showed the same LacZ activity as the strain with wild-type GoxR, suggesting that C31 is not required for GoxR activity and presumably not involved in the formation of the Fe-S cluster. This result is in accordance with the fact that C31 is not conserved in GoxR homologs of the *Acetobacteraceae* (Fig. S1). According to these data, C14, C17, C25, and C113 are likely to be involved in formation of the Fe-S cluster of GoxR. As the GoxR variants with C→A exchanges might not fold properly and are degraded, we attempted to determine the GoxR protein levels using an antiserum raised against *E. coli* FNR. However, the antiserum did not react with GoxR (data not shown).

DISCUSSION

Triggered by the finding that a shift from oxygen excess to oxygen limitation causes expression changes of about 500 genes in *G. oxydans* (21), we searched for putative oxygen-sensing transcriptional regulators and identified the GoxR protein (GOX0974) as a candidate. GoxR belongs to the FNR family of transcriptional regulators, which is part of the CRP superfamily of homodimeric transcription factors. Members of this superfamily are composed of an N-terminal

347 sensory domain and a C-terminal DNA-binding domain (25). The fumarate-nitrate-reductase
348 regulator FNR was first identified in *E. coli* and shown to regulate the expression of genes involved
349 in fumarate and nitrate respiration in dependence of oxygen (41, 42). FNR has become a paradigm
350 for oxygen-sensing transcriptional regulators (22, 26, 43). The regulatory mechanism of FNR
351 involves the assembly and degradation of an oxygen-sensitive [4Fe-4S] cluster in the N-terminal
352 domain coordinated by the cysteine residues C20, C23, C29, and C122 (*E. coli* numbering). Under
353 anoxic conditions, FNR contains a [4Fe-4S] cluster, which enables dimerization, site-specific DNA
354 binding, and transcriptional regulation (44-47). Upon oxygen-exposure, the [4Fe-4S] cluster is
355 converted to a [2Fe-2S] cluster, which results in inactivation of FNR by monomerization and
356 dissociation from DNA (48, 49). The [2Fe-2S] cluster of the monomeric FNR is completely lost
357 after prolonged oxygen exposure (50). Recently, the crystal structure of the FNR protein of
358 *Aliivibrio fischeri* was solved, which allowed a more precise description of the events occurring
359 when the [4Fe-4S] cluster is converted to the [2Fe-2S] form (51).

360 The classification of *G. oxydans* GoxR as an FNR-type regulator was initially based on sequence
361 similarity, in particular on the presence of the cysteine residues C14, C17, C25, C31, and C113 in
362 the N-terminal domain and the presence of a DNA recognition helix in the C-terminal domain with
363 an amino acid sequence very similar to the one of *E. coli* FNR (Fig.
364 S1). Experimental support for the presence of an oxygen-labile iron-sulfur cluster in GoxR was
365 obtained by the presence of a characteristic peak at 420 nm in the UV-VIS spectrum and the brown
366 to dark-green color of an anaerobically purified MBP-GoxR fusion protein. The peak disappeared
367 upon prolonged exposure to oxygen. Reporter gene assays in an *E. coli* Δfnr strain with GoxR
368 variants carrying C14A, C17A, C25A, C31A and C113A amino acid exchanges suggested that
369 C14, C17, C25, and C113 are involved in forming an iron-sulfur cluster. A notable difference

between GoxR and *E. coli* FNR is the distance between the second and third cysteine residue involved in cluster formation, which comprises five amino acids in the case of FNR, but seven in the case of GoxR (Fig. S1). This difference can be assumed to impact the properties of the iron-sulfur cluster, such as its oxygen sensitivity. FNR homologs with a seven amino acid distance between the second and third cysteine residue were previously reported (e.g. for *Bradyrhizobium japonicum* FixK1 (52) or *Rhizobium leguminosarum* FnrN (53)), but to our knowledge the biochemical properties of these proteins have not yet been studied.

FNR-type regulators are characteristic for facultative anaerobic bacteria, in which they control the transition between aerobic and anaerobic energy metabolism. The presence of an FNR homolog in *G. oxydans* is surprising, because according to current knowledge this species is not capable of anaerobic growth by respiratory or fermentative pathways and therefore considered as a strict aerobe. Consequently, the regulon of GoxR might differ from that of FNR-type regulators in facultative anaerobes. The GoxR regulon was determined by identifying the genes with altered expression in a Δ *goxR* mutant by RNA-Seq, reporter assays and enzyme activity measurements and by identifying the *in vivo*-binding sites of GoxR by ChAP-Seq. Seven genes organized in three transcriptional units were elucidated as major GoxR targets. Two of them (*cioAB*) encoding the *bd*-type ubiquinol oxidase CIO showed increased expression and two GoxR binding sites similar to the *E. coli* FNR consensus binding site TTGAT-N₄-ATCAA were found in the promoter region of *cioA* centered at positions -2.5 and -56.5 with respect to the TSS of *cioA*. Their occupation by GoxR was confirmed by the ChAP-Seq experiment, indicating that transcription of *cioAB* is directly repressed by GoxR. Repression of *cioAB* by GoxR was also confirmed by reporter gene assays, where LacZ activity was 30- to 58-fold higher in the Δ *goxR* mutant compared to the parental strain. In an *E. coli* Δ *fnr* background, expression of *lacZ* under control of the *cioA* promoter was 3-

fold higher in the absence of GoxR than in its presence, further supporting a repressor function of GoxR for *cioAB* expression. As described in the introduction, the non-proton-pumping terminal oxidase CIO has a lower oxygen affinity than the proton-pumping cytochrome *bo*₃ oxidase. Therefore, repression of the *cioAB* genes under oxygen deficiency seems reasonable, as it favors usage of oxygen by the energetically more efficient cytochrome *bo*₃ oxidase. It is interesting to note that the FNR-homolog CydR from *Azotobacter vinelandii*, like *G. oxydans* an obligately aerobic bacterium, also represses the expression of the *cydAB* genes encoding a cytochrome *bd*-type oxidase (54). Like CIO of *G. oxydans*, this oxidase from *A. vinelandii* has a low apparent *K_m* value for oxygen of 4.5 μ M (55) and its synthesis increases with oxygen supply to enable respiratory protection of the oxygen-sensitive nitrogenase (54). *G. oxydans* does not possess nitrogenase, but is confronted with conditions requiring high terminal oxidase activities due to the rapid oxidation of substrates in the periplasm by membrane-bound dehydrogenases (16).

Among the genes showing reduced mRNA levels in the Δ *goxR* mutant, the five genes of the *pnt* operon (*pntAIA2B*-GOX0313-GOX0314) were the most striking. The results of the RNA-Seq analysis were supported by reporter gene assays as well as by reduced activities of propionaldehyde reductase and hydrocinnamaldehyde reductase, which were previously shown to be catalyzed by the purified GOX0313 oxidoreductase (34). The presence of a GoxR consensus motif TTGATatccATCAA at position -41.5 with respect to the TSS of *pntA1* and the occupancy of this motif by GoxR in the ChAP-Seq experiment suggest that the *pnt* operon is directly activated by GoxR (56). What is the physiological function of the upregulation of the *pnt* operon? Under conditions of oxygen limitation, *G. oxydans* cells face the problem of insufficient NADH reoxidation, because they cannot switch to anaerobic respiration or fermentation. Loss of NADH reoxidation would result in a stop of cytoplasmic carbon source catabolism and growth. A

possibility to ensure at least a residual NADH oxidation could be the reduction of acetaldehyde to ethanol. Because *G. oxydans* lacks a functional TCA cycle, pyruvate formed either by the pentose phosphate pathway or the Entner-Doudoroff pathway is converted by pyruvate decarboxylase to acetaldehyde, which is usually further oxidized to acetate by the NADP⁺-dependent acetaldehyde dehydrogenase GOX2018 (18). Under conditions of insufficient NADH reoxidation by NADH dehydrogenase, acetaldehyde could be reduced with NADH to ethanol by the GOX0313 oxidoreductase. Purified GOX0313 protein showed the highest activity for acetaldehyde reduction to ethanol (179 U/mg), whereas the activity for NAD⁺-dependent ethanol oxidation to acetaldehyde was only 20 U/mg (34). We tested the idea that *G. oxydans* can form ethanol by incubating cells under oxygen-restricted conditions in a buffer containing glucose as carbon source and could detect the formation of small amounts of ethanol over a period of four days (Fig. 4). The Δ *goxR* mutant also formed ethanol under these conditions, but at much lower levels, in agreement with the expectation that the Δ *goxR* mutant possesses less GOX0313 activity than the parental strain (Fig. 3).

In addition to the *pnt* operon, GOX0090 was also downregulated in the Δ *goxR* mutant. The presence of a GoxR-binding motif at position -41.5 with respect to the TSS of GOX0090 and the occupancy of this site by GoxR in the ChAP-Seq experiment indicate direct transcriptional activation of this gene by GoxR. The GOX0090 protein is a homolog of YjeF of *E. coli*, which was shown to function as NAD(P)HX epimerase/dehydratase (35). NAD(P)HX (β -6-hydroxy-1,4,5,6-tetrahydronicotinamide adenine dinucleotide) is a derivative of NAD(P)H, which is formed either enzymatically by a side-reaction of glyceraldehyde 3-phosphate dehydrogenase or spontaneously and functions as an inhibitor of NAD(P)⁺-dependent enzymes, such as glucose 6-phosphate dehydrogenase or 6-phosphogluconate dehydrogenase (57, 58). *E. coli* YjeF eliminates toxic

NAD(P)HX by catalyzing the ADP-dependent dehydration of (*S*)-NAD(P)X with its C-terminal domain, while the N-terminal domain functions as an epimerase converting (*R*)-NAD(P)X to (*S*)-NAD(P)X (35). A similar function can be assumed for the GOX0090 protein of *G. oxydans*, which shows 30% sequence identity to YjeF. Because only the reduced forms, NADH and NADPH, can be hydrated, an increased demand for this repair enzyme is expected under conditions of insufficient NAD(P)H reoxidation. Recently, it was reported that YjeF might have a moonlighting function which involves vitamin B₆ (59).

The reporter gene assays and the aldehyde reductase activities suggested that GoxR is active when the cells are cultivated with 15% DO. Two features might be debated as a basis for this result. The first one relates to the very high activities of the membrane-bound dehydrogenases of *G. oxydans* in oxidizing carbon sources in the periplasm, which results in very high respiration rates. As a consequence, microaerobic or anoxic conditions are likely to prevail in the cytoplasm even when DO in the medium is still high, allowing the formation of active GoxR. Second, the oxygen-sensitivity of GoxR might be lower than that of *E. coli* FNR, for example due to the altered spacing of the third and fourth cysteine residues involved in forming the [4Fe-4S] cluster or other sequence alterations that support formation of an active GoxR dimer (46, 60). Further studies are required to compare the cytoplasmic oxygen level in *G. oxydans* with that of bacteria that do not rapidly oxidize carbon substrates in the periplasm and to determine the oxygen-responsiveness of GoxR compared to FNR.

In summary, our studies identified GoxR as an FNR-type regulator that regulates expression of genes involved in respiration and redox metabolism in *G. oxydans* as summarized in Fig. 7. It appears likely that these results are also of relevance for other acetic acid bacteria, because GoxR, the terminal oxidase CioAB, the membrane-bound transhydrogenase PntA1A2B, the

oxidoreductase GOX0313, or the NAD(P)HX epimerase/dehydratase GOX0090 (YjeF) are highly conserved in *Acetobacteraceae*.

MATERIALS AND METHODS

Materials.

Chemicals and biochemicals were obtained from Sigma-Aldrich (Taufkirchen, Germany), Carl Roth GmbH (Karlsruhe, Germany), Qiagen (Hilden, Germany), Merck (Darmstadt, Germany), Roche Diagnostics (Mannheim, Germany), Fermentas (Thermo Fisher Scientific, Germany), Finnzymes (Thermo Fisher Scientific, Germany), or Becton Dickinson GmbH (Heidelberg, Germany).

Bacterial strains, plasmids, media and growth conditions.

The bacterial strains and plasmids used in this study are listed in Table 2. The *Escherichia coli* strains were routinely cultivated in lysogeny broth (LB) or on LB agar plates at 37°C (61). For anaerobic cultivation of *E. coli* in sealed serum bottles, a minimal salts medium supplemented with 0.4% glycerol, 40 mM sodium fumarate, 20 mM trimethylamine N-oxide (TMAO), and 10% (v/v) LB broth was prepared as described (62). When required, kanamycin was added to a final concentration of 50 µg ml⁻¹. *G. oxydans* 621H and mutant strains derived thereof were cultivated in mannitol medium containing 220 mM (4% w/v) mannitol, 5 g l⁻¹ yeast extract, 2.5 g l⁻¹ MgSO₄ x 7 H₂O, 1 g l⁻¹ (NH₄)₂SO₄ and 1 g l⁻¹ KH₂PO₄. The initial pH value of the medium was 6.0. *G. oxydans* possesses a natural resistance towards cefoxitin; as a precaution to prevent bacterial contaminations, cefoxitin was added to the media at a concentration of 50 µg ml⁻¹. When required, kanamycin (50 µg ml⁻¹) was added. Precultures were grown in baffled shaking flasks at 30°C and

140 rpm. For determination of growth parameters, RNA-Seq analysis, and aldehyde reductase assays, *G. oxydans* was cultivated in 250 ml of the same medium in a bioreactor system (DASGIP, Jülich, Germany) composed of four 400-ml vessels, each equipped with electrodes for measuring the dissolved oxygen concentration (DO) and the pH. The system enabled these two parameters to be kept constant. The carbon dioxide concentration in the exhaust gas was measured continuously by an infrared spectrometer and the oxygen concentration by a zirconium dioxide sensor. The oxygen availability was kept constant at 15% DO by mixing air, O₂ and N₂. Calibration was performed by gassing with air (100% DO) and 100% N₂ (0% DO). Anaerobic conditions were achieved by gassing with 100% N₂. The agitation speed was kept constant at 900 rpm. Controlling and recording of all data as well as calculation of oxygen transfer rates (OTR) and CO₂ transfer rates (CTR) was carried out by the “Fedbatch Pro” software (DASGIP, Jülich, Germany). For oxygen limitation experiments, the bacteria were first cultivated at 15% DO to an optical density at 600 nm (OD₆₀₀) of 2.5 and then the culture was supplied with a gas mixture composed of 2% O₂/98% N₂.

General cloning methods and DNA techniques.

For DNA manipulation standard methods were used (63). For PCR, genomic DNA isolated from *G. oxydans* 621H $\Delta hsdR$ was used as template. Competent cells of *E. coli* were prepared with CaCl₂ and transformed as described (64). DNA sequencing was performed by Agowa (Berlin, Germany) or Eurofins (Ebersberg, Germany). Oligonucleotides were synthesized by Biolegio (Nijmegen, Netherlands) and are listed in Table 3.

Construction of plasmids.

For heterologous overproduction of the GoxR protein, the *goxR* gene (GOX0984) was amplified from genomic DNA of *G. oxydans* using oligonucleotides 0974_ex_ndeI_fw and 0974_ex_stopxho_rev introducing a NdeI restriction site including the ATG start codon and an XhoI site after the stop codon. After digestion with NdeI and XhoI, the PCR product was cloned into pET-TEV, a pET28b derivative carrying a sequence coding for an N-terminal hexahistidine tag followed by a recognition site for tobacco etch virus (TEV) protease and a unique NdeI restriction site. The recombinant plasmid pET-TEV-*goxR* was transferred into *E. coli* BL21(DE3) and used to overexpress *goxR*, which, however, resulted in the formation of inclusion bodies. Therefore, a second expression plasmid was constructed based on the expression vector pMal-c. The *goxR* gene including the TEV recognition site in front of the native start codon was amplified from plasmid pET-TEV-*goxR* using oligonucleotides TEV-site-Eco-fw and 0974_ex_stopxba_rev that introduced EcoRI and XbaI restriction sites. After digestion with EcoRI and XbaI the PCR product was cloned into pMal-c cut with the same enzymes. The resulting plasmid pMal-c-*goxR* encodes a 69,602 kDa fusion protein of the *E. coli* maltose binding protein without signal peptide (MBP) and GoxR linked by a TEV cleavage site between the fusion partners.

To identify cysteine residues in GoxR that are involved in the formation of the predicted [4Fe-4S] cluster and therefore important for GoxR activity, five GoxR variants were constructed. The *goxR* gene (GOX0984) was amplified from genomic DNA of *G. oxydans* using oligonucleotides 0974_ex_ndeI_fw and 0974_ex_stopxba_rev introducing a NdeI restriction site including the ATG start codon and an XbaI site after the stop codon. After digestion with XbaI, the PCR product was cloned into pTrc99a restricted with SmaI and XbaI to yield the plasmid pTrc99a-*goxR*. GoxR variants with the amino acid exchanges C14A, C17A, C25A, C31A, and C114A were constructed using the QuikChange™ Site-Directed Mutagenesis Kit (Agilent Technologies, Waldbronn,

Germany). Plasmid pTrc99a was chosen since it is compatible with the pLacZ (pBBR) reporter plasmid. The pTrc99-based plasmids and selected pLacZ-based plasmid were transferred into a Δfnr derivative of *E. coli* BW25113. This strain was constructed using *E. coli* JW1328 (BW25113 *fnr::Km^R*, Keio Collection; (65)) as parent. By expression of the Flp recombinase from plasmid pCP20 (66) the removal of the chromosomally inserted kanamycin-resistance cassette was achieved. This was necessary since the kanamycin resistance would have impeded use of the pLacZ-based reporter plasmids.

Cloning of plasmid-based transcriptional fusions of promoter regions with *lacZ*.

The activity of GoxR was tested using reporter plasmids carrying transcriptional fusions of putative target gene promoters with a promoter-less *E. coli lacZ* gene encoding β -galactosidase. The pBBR-derivative pLacZ (kindly provided by DSM Nutritional Products Ltd., Kaiseraugst, Switzerland) served as parent plasmid. The promoter regions of the selected target genes with a size of about 350 bp were amplified by PCR and cloned into pLacZ using NdeI and EcoRI restriction sites. For construction of the control plasmid pLacZ_control carrying a promoter-less *lacZ* gene, plasmid pLacZ was cut with NdeI and EcoRI, the 3'-recessive ends were filled up with Klenow polymerase and the plasmid was religated.

Transformation of *G. oxydans* by electroporation.

The cells were made competent for electroporation by inoculating 60 ml mannitol medium with 1% (v/v) of an overnight culture of the strain to be transformed. At an OD₆₀₀ of 0.8-1.2 cells from 50 ml culture were harvested by centrifugation at 4°C, washed three times with 25 ml of ice-cold 1 mM HEPES buffer pH 7.0, and then resuspended in 250 μ l 1 mM HEPES pH 7.0. The suspension

was mixed with 20 µl 75% glycerol per 100 µl cell suspension, dispensed in 50 µl aliquots, shock-frozen in liquid nitrogen, and stored at -80°C.

For electroporation, an aliquot of electro-competent cells was thawed on ice and then transferred into an electroporation cuvette with 1 mm electrode distance (VWR, Germany). After adding 100-300 ng of plasmid, the cuvette was placed in an electroporation chamber (Bio-Rad Laboratories, USA) and exposed to a pulse of 2 kV. The suspension was immediately mixed with 300 µl of electroporation medium containing per liter 80 g mannitol, 15 g yeast extract, 2.5 g MgSO₄ x 7 H₂O, 0.5 g glycerol and 1.5 g CaCl₂, pH 6, and transferred into a 15 ml Falcon tube for recovery overnight. Then the cells were plated in different dilutions on selective solid medium and incubated for 2-3 days.

Transformation of *G. oxydans* by conjugation.

The plasmid to be transferred into *G. oxydans* was first transferred into chemically competent *E. coli* S17-1. The recombinant *E. coli* S17-1 strain was cultivated in 100 ml LB medium with kanamycin to an OD₆₀₀ of 0.6 to 0.8. The *G. oxydans* recipient strain was cultivated in 100 ml mannitol medium with cefoxitin to an OD₆₀₀ 0.5-1. Then 50 ml of each culture were spun down in Falcon tubes and washed twice with 25 ml *G. oxydans* mannitol medium without cefoxitin. After the second washing step, the *G. oxydans* cells were resuspended in the smallest possible volume of mannitol medium and mixed with the *E. coli* S17-1 cells treated similarly. The suspension was spotted on a mannitol medium agar plate without antibiotics and incubated at 30°C overnight. Then the cells were scraped from the plate with 2 ml mannitol medium and different dilutions were plated on mannitol medium agar containing kanamycin and cefoxitin, which selects for *G. oxydans* cells harboring the plasmid, and incubated for 2-3 days at 30°C.

Marker-free deletion of *goxR*.

For marker-free deletion of the *goxR* gene in the *G. oxydans* genome, a two-step homologous recombination method based on plasmid pK19mobsacB was used (67), which is unable to replicate in *G. oxydans*. Please note that very efficient alternative deletion methods exist for *G. oxydans* (68), which were not yet available when the $\Delta goxR$ mutant was constructed. In a first step, the upstream and downstream regions of *goxR* were amplified by PCR using the oligonucleotide pairs 0974_f1_xba_fw/0974_f1_fus_rev and 0974_f2_pst_rev/ 0974_f2_fus_fw. The oligonucleotides 0974_f1_fus_rev and 0974_f2_fus_fw carried complementary 5'-ends, allowing fusion of the two PCR products by overlap extension PCR. The resulting 935 bp PCR product was cut with XbaI and PstI and cloned into pK19mobsacB restricted with the same enzymes. The resulting plasmid pK19mobsacB-*goxR* was transferred into *G. oxydans* by conjugation. Km^R and cefoxitin-resistant *G. oxydans* clones were isolated on mannitol medium agar plates and incubated overnight in 50 ml mannitol medium supplemented with kanamycin and cefoxitin. Then the cells were harvested, washed in mannitol medium with kanamycin, resuspended in 2 ml mannitol medium with cefoxitin, but without kanamycin, and incubated for 6-10 h at 30°C. This incubation allows a second recombination step leading either to the wild-type situation or to the desired deletion of *goxR*. The cells were then plated on mannitol medium agar plates containing cefoxitin and 10% (w/v) sucrose, the latter being toxic for cells still carrying the levansucrase gene *sacB*. Sucrose- and cefoxitin-resistant colonies that were kanamycin-sensitive were analyzed by PCR for the presence or absence of the *goxR* gene. On the one hand the *goxR* region was amplified with the oligonucleotides 0974_region_fw and 0974_region_rev, which results in a smaller PCR fragment in a $\Delta goxR$ mutant than in the wild type. With the gene specific oligonucleotides 0974_gene_fw and 0974_gene_rev,

a PCR fragment is only obtained with the wild type, but not with the $\Delta goxR$ mutant. Three $\Delta goxR$ deletion mutants were selected and stored as glycerol cultures, one of which was used for further studies.

Construction of a *G. oxydans* strain encoding GoxR with a C-terminal StrepTag.

To construct a *G. oxydans* strain genomically encoding a GoxR variant with a C-terminal StrepTag-II, the two-step homologous recombination system based on the plasmid pKOS6b was used (68). For this purpose, about 500 bp of the 3'-terminus of *goxR* without the stop codon was amplified using the oligonucleotides *goxR-strep_01_fw* and *goxR-strep_02_rev* generating a fragment with an overlap to the pKOS6b backbone and including the sequence encoding a Ser-Ala spacer and the Strep-tag (SAWSHPQFEK). The second fragment with an overlap to the Strep-tag-encoding sequence, a stop codon, about 500 bp downstream of *goxR*, and an overlap to the pKOS6b backbone vector was obtained with *goxR-strep_03_fw*/ *goxR-strep_04_rev*. The two PCR products and the digested pKOS6b plasmid (EcoRI, XbaI) were assembled using Gibson assembly (69). The resulting plasmid pKOS6b-*goxR-strep* was used to transform *E. coli* DH5 α . Positive clones were selected by colony PCR (pKOS6b_seq_fw/pKOS6b_seq_rev) and isolated plasmids were verified by sequencing. Then pKOS6b-*goxR-strep* was transferred into the strain *E. coli* S17-1 for conjugation into *G. oxydans* as described above. Cefoxitin and Km^R-resistant clones were isolated on agar plates and incubated overnight in 1 ml recombination medium (40 g l⁻¹ mannitol, 2.5 g l⁻¹ yeast extract, 1 g l⁻¹ MgSO₄ x 7 H₂O) supplemented with both kanamycin and cefoxitin to a final concentration of 50 μ g ml⁻¹. Cells of the overnight cultures were harvested, washed twice with recombination medium, resuspended in 3 ml recombination medium with cefoxitin and then incubated for ca. 6 h at 30°C. Positive clones containing the modified *goxR* gene but not the vector

backbone, were selected on agar plates with cefoxitin and 60 µg/µl 5'-fluorocytosine. Correct integration into the *goxR* locus was confirmed by sequencing of the colony PCR product obtained with the oligonucleotides *goxR-strep_seq_fw* and *goxR-strep_seq_rev*. The resulting strain was named *G. oxydans* 621H::*goxR-strep*.

RNA sequencing and differential gene expression analysis.

RNA was isolated using the RNeasy Kit (Qiagen, Hilden, Germany) and quality-checked using the Agilent Tape station 2200 (Agilent Technologies, Waldbronn, Germany) with the RNA ScreenTape according to the manufacturer's instructions. To remove rRNA of all samples, the RiboMinus Transcriptome Isolation Kit for Yeast and Bacteria (Invitrogen, Carlsbad, USA) was used. rRNA-depleted RNA was precipitated with ethanol overnight at -20°C. The pellet was dissolved in 7 µl nuclease-free water. Successful depletion was verified with the Tape Station using Agilent's High Sensitivity RNA ScreenTape. Sequencing libraries were generated with the NEBNext Ultra II Directional RNA Library Prep Kit for Illumina (New England Biolabs, Frankfurt, Germany) following the protocol for rRNA-depleted RNA using 11 cycles for PCR amplification of adaptor-ligated DNA. For quantification of the final cDNA libraries, the KAPA library quantification Kit from KapaBiosystems (Roche, Unterhaching, Germany) was used following the manufacturer's instructions. The qPCR itself was conducted on a qTOWER 2.2 (Analytik Jena, Jena, Germany). Two or four cDNA samples were pooled and then paired-end (2 x 75 cycles) sequenced on a MiSeq platform (Illumina, Munich, Germany) with the MiSeq Reagent Kit v3 (150-cycle). Read processing and strand-specific mapping to the *G. oxydans* 621H reference genome (NC_006672.1-NC_006677.1) was carried out with the CLC Genomics Workbench

(Qiagen, Aarhus, Denmark). Subsequent empirical analysis of differential gene expression for three biological replicates was performed with edgeR (70).

ChAP-Seq analysis for the identification of *in vivo* GoxR binding sites.

For preparation of ChAP-Seq samples, the strain *G. oxydans* 621H::*goxR-strep* was used. A preculture was inoculated in 15 ml mannitol medium and incubated for 8 h at 30°C. Subsequently, 1 ml of the first preculture was transferred into 50 ml mannitol medium. After cultivation overnight, this second preculture was used to inoculate the main culture (1 l in a 5 l baffled Erlenmeyer flask) to an OD₆₀₀ of 0.5. The culture was incubated at 30°C and 130 rpm. In the late exponential phase (OD₆₀₀ ca. 2.8), cells were harvested by centrifugation and washed once in 40 ml PBS (137 mM NaCl, 2.7 mM KCl, 1.5 mM KH₂PO₄, 8 mM Na₂HPO₄, pH 7.4). Afterwards, the cell pellet was resuspended in 20 ml PBS with 1% (v/v) formaldehyde incubated for 20 min at room temperature to crosslink the Strep-tagged GoxR protein to DNA. To stop the crosslinking, glycine was added to a final concentration of 125 mM followed by incubation for 5 min at room temperature. Afterwards, cells were washed twice with 40 ml buffer A (100 mM Tris-HCl, pH 8.0, 1 mM EDTA) and pellets were stored overnight at -80°C. Cell disruption, sonication of the DNA, purification of DNA bound to Strep-tagged GoxR, and the final DNA purification after digestion of protein was performed as described (71). The obtained DNA fragments were prepared for sequencing using the NEBNext Ultra II DNA Library Prep Kit for Illumina following the manufacturer's protocol for DNA fragments without size selection. Adapter-ligated DNA was amplified by using 15 PCR cycles. Quantification of the resulting libraries was performed with the KAPA library quantification kit as described above and sequenced on a MiSeq (Illumina) using paired-end sequencing with a read-length of 2 × 150 bases. Mapping of the sequencing data and

peak detection was done with an analysis pipeline described recently for another transcriptional regulator (72). Briefly, mapping of the reads to the *G. oxydans* 621H reference genome (NC_006672.1-NC_006677.1) was done using Bowtie2 (73) in local alignment mode with the following parameters: "-D 20 -R 3 -N 0 -L 20 -i S,1,0.50". Based on the genomic read coverage peaks were detected using convolution with second order gaussian kernel. The width of each peak was defined as the distance between two points with a coverage lower than 1/2 of the maximal peak height. Peak intensities were calculated by normalization of the highest read coverage to the average coverage of non-peak genomic area.

Determination of transcriptional start sites by 5'-RACE.

To determine the transcriptional start sites of *cioA* and *pntA1*, The 5'-RACE method was performed with 1 µg RNA isolated from the *G. oxydans* parent strain and a 5'/3'-RACE kit (2nd generation) according to the protocol of the supplier (Roche Diagnostics, Mannheim, Germany). PCR fragments resulting from amplification with the PCR Anchor Primer and the gene-specific SP2 or SP3 primers (see Table 3) were subjected to agarose gel electrophoresis, isolated, and sequenced. In the case of *cioA* (GOX028) and *pntA1* (GOX0310), two and five sequences allowed the determination of the TSSs, respectively (Fig. S2).

Overproduction and purification of GoxR.

The expression plasmid pMal-c-*goxR* was transferred into *E. coli* BL21(DE3) as expression host. Cultures were grown at 37°C in LB medium inoculated with 1% (v/v) of an overnight preculture. At an OD₆₀₀ of 0.5 to 0.8 expression of the target gene was induced by addition of 0.5 mM IPTG and the culture was subsequently incubated overnight at 16°C and 120 rpm.

Subsequently, 125 ml of the culture was incubated overnight at 300 rpm and 4°C under anaerobic conditions in the presence of 10 mM ferric ammonium citrate and 10 mM L-cysteine hydrochloride. All following steps were performed in an anaerobic chamber. Cells were harvested by centrifugation for 15 min at 4°C. 1 g cells (wet weight) was resuspended in 2 ml buffer A (20 mM Tris/HCl pH 7.4, 200 mM NaCl, 1 mM EDTA, 5 mM DTT) supplemented with Complete protease inhibitor cocktail (Roche Diagnostics) and the cells were disrupted in 2 ml screw-cap vials containing glass beads (0.1 mm diameter; 4 g glass beads per g cell wet weight) using a FastPrep disruptor (Fermentas). The cells were disrupted for 20 s and after chilling for three minutes on ice for an additional 15 s. The suspension was centrifuged for 20 min at 13,000 rpm in a table-top centrifuge and the cell-free extract was collected in a vial. For purification of the MBP-GoxR fusion protein, the cell-free extract was loaded onto a 1.5-ml column with amylose resin (New England Biolabs) and equilibrated with buffer A. After washing with several column volumes of buffer A, MBP-GoxR was eluted with buffer A supplemented with 10 mg ml⁻¹ maltose monohydrate using fraction volumes of 0.5 ml. The purity of the isolated MBP-GoxR protein was checked by SDS-polyacrylamide gel electrophoresis (SDS-PAGE). Fraction 3 was used for recording a UV/Vis spectrum from 200-900 nm using a UV-2450 spectrophotometer (Shimadzu Corporation, Kyoto, Japan), as it had the most intensive color. For this purpose, the MBP-GoxR fraction was filled into a quartz cuvette in the anaerobic chamber and sealed with a rubber stopper. For oxidation of MalE-GoxR, the protein solution was incubated under aerobic condition with shaking on ice for seven hours, before recording the UV-Vis spectrum.

β-Galactosidase assays.

The pLacZ derivatives carrying various promoter regions (Table 2) were transferred into the *G. oxydans* parental strain and the $\Delta goxR$ mutant and cultivated as described in the results section. For analyzing the impact of selected cysteine residues in GoxR for repression of the *cioA* promoter, *E. coli* BW23113 Δfnr transformed with pLacZ_*cioA* and one of the pTrc99a-*goxR* plasmids was cultivated anaerobically in minimal salts medium. Gene expression was induced by addition of 0.05 mM IPTG and the cultures were subsequently incubated without shaking at 37°C until reaching an OD₆₀₀ of 0.5-0.6. Cells were harvested by centrifugation at 4°C for 10 min and then used for β -galactosidase assays. The β -galactosidase activity were determined as described (74) by measuring the formation of *o*-nitrophenol from 2-nitrophenyl- β -D-galactopyranoside (ONPG) photometrically at 420 nm and 28°C for *G. oxydans* and *E. coli*.

Determination of NADH-dependent aldehyde reductase activity.

The parent strain and the $\Delta goxR$ mutant were cultivated at 15% DO and 0% DO in a bioreactor system as described above. The cells were harvested by centrifugation at 8,600 g and 4°C for 10 min. The cells were washed with 50 mM Tris-HCl pH 7.5, resuspended in the same buffer and lysed by passing them twice through a French pressure cell press (American Instrument Company, Silver Spring, MD, USA) at 1,100 kg cm⁻². After ultracentrifugation at 160,000 g and 4°C for 1 h, the supernatant was obtained and used as the soluble fraction. NADH-dependent aldehyde reductase activity in the soluble fraction was determined spectrophotometrically at 340 nm as described (34). 10 mM propionaldehyde or 1 mM hydrocinnamaldehyde were used as substrates. Hydrocinnamaldehyde was dissolved in dimethylsulfoxide at 100 mM prior to enzyme assay. 1 Unit of enzyme activity was defined as 1 μ mol substrate reduced per min.

Ethanol production under oxygen-depleted conditions.

Cells of the parental strain and the ΔgoxR mutant were cultivated in shake flasks with mannitol medium under vigorous shaking. When the cells had reached the stationary phase, they were harvested by centrifugation, washed and resuspended in 50 mM MOPS buffer adjusted with KOH to pH 6.0. The density of the cell suspension was adjusted to an OD₆₀₀ of 1. 6 ml of the cell suspension and 6 ml of a 44 mM glucose solution were mixed in a 15 ml Falcon tube. The free space in the tube was flushed with argon gas and the tube immediately closed tightly with a cap. The tube was shaken horizontally at 120 rpm at 30°C for the indicated times. Ethanol in the cell-free supernatant of the cell suspensions was determined by gas chromatography (GC) using an Agilent 7890A gas chromatograph (Agilent Technologies, Waldbronn, Germany) as described previously (75). Calibration was performed with ethanol solutions from 0.05 to 3.2 mM as an external standard. The detection limit of ethanol was 0.1 mM under the conditions used. Butanol was added to the samples as an internal standard at a concentration of 2 mM. Concentrations were calculated from peak areas using calibration with external ethanol and internal butanol standards.

Data availability statement.

Bacterial strains and plasmids described in this study are available from the corresponding author upon request. The RNA-Seq data were deposited in the GEO database with the accession number GSE147810. The ChAP-Seq data were deposited in the GEO database with the accession number GSE159734.

FUNDING INFORMATION

This work was supported by the German Ministry of Education and Research (BMBF) within the GenoMik-Transfer program (grant 0315632D to MB) and MEXT KAKENHI grant number 26450095 to TY. TY thanks to Yamaguchi University for encouraging collaboration with Forschungszentrum Jülich under the International Collaborative Research project.

ACKNOWLEDGEMENTS

We are most grateful to Prof. Gottfried Uden (Universität Mainz) for sharing his knowledge on FNR proteins and for providing a working space for experiments with GoxR under anoxic conditions. Many thanks go to Stephanie Nilkens from Gottfried Uden's lab, who introduced Stefanie Schweikert into anaerobic work. We also thank DSM Nutritional Products (Kaiseraugst, Switzerland) for financial support and Dietmar Laudert, Günter Pappenberger and Hans-Peter Hohmann (DSM Nutritional Products) for their scientific input and their continued disposition for discussion.

772 REFERENCES

- 773 1. Kersters K, Lisdiyanti P, Komagata K, Swings J. 2006. The family *Acetobacteriaceae*: The genera
774 *Acetobacter*, *Acidomonas*, *Asaia*, *Gluconacetobacter*, *Gluconobacter* and *Kozakia*, p p. 163-200. In
775 Dworkin M, Falkow S, Rosenberg E, Schleifer K-H, Stackebrandt E (ed), *The Prokaryotes*, 3rd
776 edition ed, vol 5. Springer-Verlag, Heidelberg
- 777 2. Pappenberger G, Hohmann HP. 2014. Industrial production of L-ascorbic Acid (vitamin C) and D-
778 isoascorbic acid. *Adv Biochem Eng Biotechnol* 143:143-188.
- 779 3. Schedel M. 2000. Regioselective oxidation of aminosorbitol with *Gluconobacter oxydans*, a key
780 reaction in the industrial synthesis of 1-deoxynojirimycin, p 296-308. In Kelly DR (ed),
781 *Biotransformations II*, 2nd edition ed. Wiley-VCH, Weinheim.
- 782 4. Bremus C, Herrmann U, Bringer-Meyer S, Sahm H. 2006. The use of microorganisms in L-ascorbic
783 acid production. *J Biotechnol* 124:196-205.
- 784 5. Deppenmeier U, Hoffmeister M, Prust C. 2002. Biochemistry and biotechnological applications of
785 *Gluconobacter* strains. *Appl Microbiol Biotechnol* 60:233-242.
- 786 6. Raspor PP, Goranovič D. 2008. Biotechnological applications of acetic acid bacteria. *Crit Rev*
787 *Biotechnol* 28:101-124.
- 788 7. Saichana N, Matsushita K, Adachi O, Frébortova I, Frébortova J. 2015. Acetic acid bacteria: A group of
789 bacteria with versatile biotechnological applications. *Biotechnol Adv* 33:1260-1271.
- 790 8. Richhardt J, Luchterhand B, Bringer S, Büchs J, Bott M. 2013. Evidence for a key role of
791 cytochrome *bo*₃ oxidase in respiratory energy metabolism of *Gluconobacter oxydans*. *J Bacteriol*
792 195:4210-4220.
- 793 9. Ameyama M, Matsushita K, Shinagawa E, Adachi O. 1987. Sugar-oxidizing respiratory chain of
794 *Gluconobacter suboxydans*. Evidence for a branched respiratory chain and characterization of
795 respiratory chain-linked cytochromes. *Agric Biol Chem* 51:2943-2950.
- 796 10. Mogi T, Ano Y, Nakatsuka T, Toyama H, Muroi A, Miyoshi H, Migita CT, Ui H, Shiomi K, Omura
797 S, Kita K, Matsushita K. 2009. Biochemical and spectroscopic properties of cyanide-insensitive
798 quinol oxidase from *Gluconobacter oxydans*. *J Biochem* 146:263-271.
- 799 11. Miura H, Mogi T, Ano Y, Migita CT, Matsutani M, Yakushi T, Kita K, Matsushita K. 2013.
800 Cyanide-insensitive quinol oxidase (CIO) from *Gluconobacter oxydans* is a unique terminal oxidase
801 subfamily of cytochrome *bd*. *J Biochem* 153:535-545.
- 802 12. Rice CW, Hempfling WP. 1978. Oxygen-limited continuous culture and respiratory energy
803 conservation in *Escherichia coli*. *J Bacteriol* 134:115-124.
- 804 13. Hanke T, Nöh K, Noack S, Polen T, Bringer S, Sahm H, Wiechert W, Bott M. 2013. Combined
805 fluxomics and transcriptomics analysis of glucose catabolism via a partially cyclic pentose phosphate
806 pathway in *Gluconobacter oxydans* 621H. *Appl Environ Microbiol* 79:2336-2348.
- 807 14. Richhardt J, Bringer S, Bott M. 2012. Mutational analysis of the pentose phosphate and Entner-
808 Doudoroff pathways in *Gluconobacter oxydans* reveals improved growth of a $\Delta edd \Delta eda$ mutant on
809 mannitol. *Appl Environ Microbiol* 78:6975-6986.
- 810 15. Richhardt J, Bringer S, Bott M. 2013. Role of the pentose phosphate pathway and the Entner-
811 Doudoroff pathway in glucose metabolism of *Gluconobacter oxydans* 621H. *Appl Microbiol*
812 *Biotechnol* 97:4315-4323.
- 813 16. Prust C, Hoffmeister M, Liesegang H, Wiezer A, Fricke WF, Ehrenreich A, Gottschalk G,
814 Deppenmeier U. 2005. Complete genome sequence of the acetic acid bacterium *Gluconobacter*
815 *oxydans*. *Nat Biotechnol* 23:195-200.
- 816 17. Kiefler I, Bringer S, Bott M. 2015. SdhE-dependent formation of a functional *Acetobacter*
817 *pasteurianus* succinate dehydrogenase in *Gluconobacter oxydans* - a first step toward a complete
818 tricarboxylic acid cycle. *Appl Microbiol Biotechnol* 99:9147-9160.

18. Krajewski V, Simić P, Mouncey NJ, Bringer S, Sahm H, Bott M. 2010. Metabolic engineering of *Gluconobacter oxydans*: improvement of growth rate and growth yield from glucose by elimination of gluconate formation. *Appl Environm Microbiol* 76:4369-4376.
19. Kiefler I, Bringer S, Bott M. 2017. Metabolic engineering of *Gluconobacter oxydans* 621H for increased biomass yield. *Appl Microbiol Biotechnol* 101:5453-5467.
20. Kranz A, Vogel A, Degner U, Kiefler I, Bott M, Usadel B, Polen T. 2017. High precision genome sequencing of engineered *Gluconobacter oxydans* 621H by combining long nanopore and short accurate Illumina reads. *J Biotechnol* doi:10.1016/j.jbiotec.2017.04.016.
21. Hanke T, Richhardt J, Polen T, Sahm H, Bringer S, Bott M. 2012. Influence of oxygen limitation, absence of the cytochrome *bc*₁ complex and low pH on global gene expression in *Gluconobacter oxydans* 621H using DNA microarray technology. *J Biotechnol* 157:359-372.
22. Spiro S, Guest JR. 1990. FNR and its role in oxygen-regulated gene expression in *Escherichia coli*. *FEMS Microbiol Rev* 6:399-428.
23. Kiley PJ, Beinert H. 1999. Oxygen sensing by the global regulator, FNR: the role of the iron-sulfur cluster. *FEMS Microbiol Rev* 22:341-352.
24. Unden G, Achebach S, Holighaus G, Tran HG, Wackwitz B, Zeuner Y. 2002. Control of FNR function of *Escherichia coli* by O₂ and reducing conditions. *J Mol Microbiol Biotechnol* 4:263-8.
25. Körner H, Soça HJ, Zumft WG. 2003. Phylogeny of the bacterial superfamily of Crp-Fnr transcription regulators: exploiting the metabolic spectrum by controlling alternative gene programs. *FEMS Microbiol Rev* 27:559-592.
26. Green J, Crack JC, Thomson AJ, LeBrun NE. 2009. Bacterial sensors of oxygen. *Curr Opin Microbiol* 12:145-151.
27. Fleischhacker AS, Kiley PJ. 2011. Iron-containing transcription factors and their roles as sensors. *Curr Opin Chem Biol* 15:335-341.
28. Mettert EL, Kiley PJ. 2015. Fe-S proteins that regulate gene expression. *Biochim Biophys Acta* 1853:1284-1293.
29. Unden G, Nilkens S, Singenstreu M. 2013. Bacterial sensor kinases using Fe-S cluster binding PAS or GAF domains for O₂ sensing. *Dalton Trans* 42:3082-3087.
30. Gilles-Gonzalez MA, Gonzalez G. 2005. Heme-based sensors: defining characteristics, recent developments, and regulatory hypotheses. *J Inorg Biochem* 99:1-22.
31. Altschul SF, Gish W, Miller W, Myers EW, Lipman DJ. 1990. Basic local alignment search tool. *J Mol Biol* 215:403-410.
32. Melville SB, Gunsalus RP. 1990. Mutations in *fnr* that alter anaerobic regulation of electron transport-associated genes in *Escherichia coli*. *J Biol Chem* 265:18733-18736.
33. Jackson JB, Leung JH, Stout CD, Schurig-Briccio LA, Gennis RB. 2015. Review and Hypothesis. New insights into the reaction mechanism of transhydrogenase: Swivelling the dIII component may gate the proton channel. *FEBS Lett* 589:2027-2033.
34. Schweiger P, Gross H, Zeiser J, Deppenmeier U. 2013. Asymmetric reduction of diketones by two *Gluconobacter oxydans* oxidoreductases. *Appl Microbiol Biotechnol* 97:3475-3484.
35. Marbaix AY, Noel G, Detroux AM, Vertommen D, Van Schaftingen E, Linster CL. 2011. Extremely conserved ATP- or ADP-dependent enzymatic system for nicotinamide nucleotide repair. *J Biol Chem* 286:41246-41252.
36. Myers KS, Yan H, Ong IM, Chung D, Liang K, Tran F, Keles S, Landick R, Kiley PJ. 2013. Genome-scale analysis of *Escherichia coli* FNR reveals complex features of transcription factor binding. *PLoS Genet* 9:e1003565.
37. Grant CE, Bailey TL, Noble WS. 2011. FIMO: scanning for occurrences of a given motif. *Bioinformatics* 27:1017-1018.
38. Bailey TL, Williams N, Misleh C, Li WW. 2006. MEME: discovering and analyzing DNA and protein sequence motifs. *Nucleic Acids Res* 34:W369-373.

- 868 39. Kranz A, Busche T, Vogel A, Usadel B, Kalinowski J, Bott M, Polen T. 2018. RNAseq analysis of
869 α -proteobacterium *Gluconobacter oxydans* 621H. BMC Genomics 19:24.
- 870 40. Guest JR, Green J, S. IA, Spiro S. 1996. The FNR modulon and FNR-regulated gene expression, p
871 317-342. In Lin ECC, Lynch AS (ed), Regulation of gene expression in *Escherichia coli*. R. G.
872 Landes & Co., Austin, TX.
- 873 41. Shaw DJ, Guest JR. 1982. Amplification and product identification of the *fnr* gene of *Escherichia*
874 *coli*. J Gen Microbiol 128:2221-2228.
- 875 42. Unden G, Guest JR. 1985. Isolation and characterization of the Fnr protein, the transcriptional
876 regulator of anaerobic electron transport in *Escherichia coli*. Eur J Biochem 146:193-199.
- 877 43. Kiley PJ, Beinert H. 1998. Oxygen sensing by the global regulator, FNR: the role of the iron-sulfur
878 cluster. FEMS Microbiol Rev 22:341-352.
- 879 44. Khoroshilova N, Beinert H, Kiley PJ. 1995. Association of a polynuclear iron-sulfur center with a
880 mutant FNR protein enhances DNA binding. Proc Natl Acad Sci USA 92:2499-2503.
- 881 45. Green J, Bennett B, Jordan P, Ralph ET, Thomson AJ, Guest JR. 1996. Reconstitution of the [4Fe-
882 4S] cluster in FNR and demonstration of the aerobic-anaerobic transcription switch *in vitro*. Biochem
883 J 316 887-892.
- 884 46. Lazazzera BA, Bates DM, Kiley PJ. 1993. The activity of the *Escherichia coli* transcription factor
885 FNR is regulated by a change in oligomeric state. Genes Dev 7:1993-2005.
- 886 47. Lazazzera BA, Beinert H, Khoroshilova N, Kennedy MC, Kiley PJ. 1996. DNA binding and
887 dimerization of the Fe-S-containing FNR protein from *Escherichia coli* are regulated by oxygen. J
888 Biol Chem 271:2762-2768.
- 889 48. Crack JC, Green J, Cheesman MR, Le Brun NE, Thomson AJ. 2007. Superoxide-mediated
890 amplification of the oxygen-induced switch from [4Fe-4S] to [2Fe-2S] clusters in the transcriptional
891 regulator FNR. Proc Natl Acad Sci USA 104:2092-2097.
- 892 49. Khoroshilova N, Popescu C, Munck E, Beinert H, Kiley PJ. 1997. Iron-sulfur cluster disassembly in
893 the FNR protein of *Escherichia coli* by O₂: [4Fe-4S] to [2Fe-2S] conversion with loss of biological
894 activity. Proc Natl Acad Sci USA 94:6087-6092.
- 895 50. Sutton VR, Stubna A, Patschkowski T, Munck E, Beinert H, Kiley PJ. 2004. Superoxide destroys the
896 [2Fe-2S]²⁺ cluster of FNR from *Escherichia coli*. Biochemistry 43:791-798.
- 897 51. Volbeda A, Darnault C, Renoux O, Nicolet Y, Fontecilla-Camps JC. 2015. The crystal structure of
898 the global anaerobic transcriptional regulator FNR explains its extremely fine-tuned monomer-dimer
899 equilibrium. Sci Adv 1:e1501086.
- 900 52. Anthamatten D, Scherb B, Hennecke H. 1992. Characterization of a *fixLJ*-regulated *Bradyrhizobium*
901 *japonicum* gene sharing similarity with the *Escherichia coli fnr* and *Rhizobium meliloti fixK* genes. J
902 Bacteriol 174:2111-2120.
- 903 53. Gutierrez D, Hernando Y, Palacios JM, Imperial J, Ruiz-Argueso T. 1997. FnrN controls symbiotic
904 nitrogen fixation and hydrogenase activities in *Rhizobium leguminosarum* biovar *viciae* UPM791. J
905 Bacteriol 179:5264-5270.
- 906 54. Wu G, Cruz-Ramos H, Hill S, Green J, Sawers G, Poole RK. 2000. Regulation of cytochrome *bd*
907 expression in the obligate aerobe *Azotobacter vinelandii* by CydR (Fnr). Sensitivity to oxygen,
908 reactive oxygen species, and nitric oxide. J Biol Chem 275:4679-4686.
- 909 55. D'mello R, Hill S, Poole RK. 1994. Determination of the oxygen affinities of terminal oxidases in
910 *Azotobacter vinelandii* using the deoxygenation of oxyleghemoglobin and oxymyoglobin -
911 cytochrome *bd* is a low-affinity oxidase. Microbiology 140:1395-1402.
- 912 56. Mettert EL, Kiley PJ. 2018. Reassessing the structure and function relationship of the O₂ sensing
913 transcription factor FNR. Antioxid Redox Signal 29:1830-1840.
- 914 57. Yoshida A, Dave V. 1975. Inhibition of NADP-dependent dehydrogenases by modified products of
915 NADPH. Arch Biochem Biophys 169:298-303.
- 916 58. Acheson SA, Kirkman HN, Wolfenden R. 1988. Equilibrium of 5,6-hydration of NADH and
917 mechanism of ATP-dependent dehydration. Biochemistry 27:7371-7375.

59. Niehaus TD, Elbadawi-Sidhu M, Huang L, Prunetti L, Gregory JF, 3rd, de Crecy-Lagard V, Fiehn O, Hanson AD. 2018. Evidence that the metabolite repair enzyme NAD(P)HX epimerase has a moonlighting function. *Biosci Rep* 38:BSR20180223.
60. Kiley PJ, Reznikoff WS. 1991. Fnr mutants that activate gene expression in the presence of oxygen. *J Bacteriol* 173:16-22.
61. Bertani G. 1951. Studies on lysogenesis. I. The mode of phage liberation by lysogenic *Escherichia coli*. *J Bacteriol* 62:293-300.
62. Constantinidou C, Hobman JL, Griffiths L, Patel MD, Penn CW, Cole JA, Overton TW. 2006. A reassessment of the FNR regulon and transcriptomic analysis of the effects of nitrate, nitrite, NarXL, and NarQP as *Escherichia coli* K12 adapts from aerobic to anaerobic growth. *J Biol Chem* 281:4802-4815.
63. Sambrook J, Russell D. 2001. *Molecular Cloning. A Laboratory Manual*, 3rd ed. Cold Spring Harbor Laboratory Press, Cold Spring Harbor, New York.
64. Hanahan D, Jessee J, Bloom FR. 1991. Plasmid transformation of *Escherichia coli* and other bacteria. *Meth Enzymol* 204:63-113.
65. Baba T, Ara T, Hasegawa M, Takai Y, Okumura Y, Baba M, Datsenko KA, Tomita M, Wanner BL, Mori H. 2006. Construction of *Escherichia coli* K-12 in-frame, single-gene knockout mutants: the Keio collection. *Mol Syst Biol* 2:2006.0008.
66. Cherepanov PP, Wackernagel W. 1995. Gene disruption in *Escherichia coli*: Tc^R and Km^R cassettes with the option of FLP-catalyzed excision of the antibiotic-resistance determinant. *Gene* 158:9-14.
67. Schäfer A, Tauch A, Jäger W, Kalinowski J, Thierbach G, Pühler A. 1994. Small mobilizable multipurpose cloning vectors derived from the *Escherichia coli* plasmids pK18 and pK19 - Selection of defined deletions in the chromosome of *Corynebacterium glutamicum*. *Gene* 145:69-73.
68. Kostner D, Peters B, Mientus M, Liebl W, Ehrenreich A. 2013. Importance of *codB* for new *codA*-based markerless gene deletion in *Gluconobacter* strains. *Appl Microbiol Biotechnol* 97:8341-8349.
69. Gibson DG, Young L, Chuang RY, Venter JC, Hutchison CA, Smith HO. 2009. Enzymatic assembly of DNA molecules up to several hundred kilobases. *Nat Meth* 6:343-345.
70. Robinson MD, McCarthy DJ, Smyth GK. 2010. edgeR: a Bioconductor package for differential expression analysis of digital gene expression data. *Bioinformatics* 26:139-140.
71. Pfeifer E, Hünnefeld M, Popa O, Polen T, Kohlheyer D, Baumgart M, Frunzke J. 2016. Silencing of cryptic prophages in *Corynebacterium glutamicum*. *Nucleic Acids Res* 44:10117-10131.
72. Keppel M, Hünnefeld M, Filipchuk A, Viets U, Davoudi CF, Krüger A, Mack C, Pfeifer E, Polen T, Baumgart M, Bott M, Frunzke J. 2020. HrrSA orchestrates a systemic response to heme and determines prioritization of terminal cytochrome oxidase expression. *Nucleic Acids Res* 48:6547-6562.
73. Langmead B, Salzberg SL. 2012. Fast gapped-read alignment with Bowtie 2. *Nat Methods* 9:357-359.
74. Miller JH. 1992. *A short course in bacterial genetics: a laboratory manual and handbook for Escherichia coli and related bacteria*. Cold Spring Harbor Laboratory Press, Cold Spring Harbor, New York.
75. Witthoff S, Mühlroth A, Marienhagen J, Bott M. 2013. C1 metabolism in *Corynebacterium glutamicum*: an endogenous pathway for oxidation of methanol to carbon dioxide. *Appl Environ Microbiol* 79:6974-6983.
76. Simon R, Priefer U, Pühler A. 1983. A broad host range mobilization system for *in vivo* genetic-engineering-transposon mutagenesis in Gram-negative bacteria. *Bio-Technol* 1:784-791.
77. Bussmann M, Baumgart M, Bott M. 2010. RosR (Cg1324), a hydrogen peroxide-sensitive MarR-type transcriptional regulator of *Corynebacterium glutamicum*. *J Biol Chem* 285:29305-29318.
78. Amann E, Ochs B, Abel KJ. 1988. Tightly regulated tac promoter vectors useful for the expression of unfused and fused proteins in *Escherichia coli*. *Gene* 69:301-315.

TABLE 1 Genes showing altered expression in the deletion mutant *G. oxydans* Δ *goxR* compared to the parent *G. oxydans* strain 20 minutes after shifting from oxygen excess (15% DO) to oxygen limitation (0% DO)^{1,2}.

Locus tag	Gene ³	Annotation	Fold change RNAseq Δ <i>goxR</i> /parent strain	p- value
Respiration and metabolism				
GOX0278	<i>cioA</i>	Terminal oxidase CIO, subunit I	6.60	0.001
GOX0279	<i>cioB</i>	Terminal oxidase CIO, subunit II	4.66	0.009
GOX0090		putative ADP-dependent NAD(P)HX epimerase/dehydratase	0.40	0.05
GOX0310	<i>pntA1</i>	Transhydrogenase subunit α 1	0.11	<0.001
GOX0311	<i>pntA2</i>	Transhydrogenase subunit α 2	0.11	0.003
GOX0312	<i>pntB</i>	Transhydrogenase subunit β	0.19	0.010
GOX0313		Alcohol:NAD ⁺ oxidoreductase	0.15	<0.00<
GOX0314		Probable alcohol:NAD(P) ⁺ oxidoreductase	0.36	0.06
Regulation				
GOX0974	<i>goxR</i>	GoxR, FNR-like transcriptional regulator	0.02	<0.001
Motility				
GOX0424	<i>fliF</i>	Flagellar MS-ring protein	0.44	0.022
GOX0425	<i>flgG</i>	Flagellar basal-body modification protein FlgG	0.38	0.018
GOX0426	<i>fliK</i>	put. flagellar hook length control protein FliK	0.27	0.02
GOX0787	<i>flaB</i>	Flagellin B	0.34	0.028
GOX0788	<i>flaF</i>	Flagellin assembly protein	0.35	0.005
GOX1528	<i>flgB</i>	Flagellar basal-body rod protein FlgB	0.36	0.017

¹The strains were cultivated in a bioreactor in mannitol medium pH 6 and 15% DO to an OD₆₀₀ of 2.5. Then the gassing was changed to 2% O₂/98% N₂, resulting in a measured DO of 0%. 20 min after the switch cells were harvested and used for RNA isolation.

² Gene expression was determined by RNAseq analysis as described in Materials and Methods. Genes with an mRNA ratio ≥ 2.0 (lower ones allowed in the case of operons) or ≤ 0.5 (higher ones allowed in the case of operons) and a *p*-value of ≤ 0.05 are listed. The data shown represent mean values from three biological replicates.

³ The genes were grouped into functional categories within which they were ordered according to their locus tag.

TABLE 2 Bacterial strains, plasmids used in this work

Bacterial strain or plasmid	Description	Reference or source
Strains		
<i>G. oxydans</i> 621H	Type strain	DMSZ
<i>G. oxydans</i> $\Delta hsdR$	621H $\Delta hsdR$; <i>hsdR</i> (GOX2567) encodes a type I restriction enzyme and is located on plasmid pGOX1	This work
<i>G. oxydans</i> $\Delta goxR$	621H $\Delta hsdR$ $\Delta goxR$; <i>goxR</i> (GOX0974) codes for an FNR-type transcriptional regulator	This work
<i>G. oxydans</i> 621H:: <i>goxR-strep</i>	621H variant encoding a GoxR variant with a C-terminal Strep-Tag at the native genomic locus	This work
<i>E. coli</i> DH5 α	<i>fhuA2</i> Δ (<i>argF-lacZ</i>)U169 <i>phoA glnV44</i> Φ 80 Δ (<i>lacZ</i>)M15 <i>gyrA96 recA1 relA1 endA1 thi-1 hsdR17</i>	(64)
<i>E. coli</i> BL21 Star (DE3)	F ⁻ <i>ompT hsdS_B(r_B⁻, m_B⁻) gal dcm rne131</i> (DE3)	Invitrogen
<i>E. coli</i> S17-1	$\Delta recA$, <i>endA1</i> , <i>hsdR17</i> , <i>supE44</i> , <i>thi-1</i> , <i>tra</i> ⁺	(76)
<i>E. coli</i> BW25113 <i>fnr::kan^R</i>	<i>rrnB3</i> , $\Delta lacZ4787$, <i>hsdR514</i> , Δ (<i>araBAD</i>)567, Δ (<i>rhaBAD</i>)568, <i>rph-1</i> , <i>fnr::Kan^R</i>	(65)
<i>E. coli</i> BW25113 Δfnr	<i>rrnB3</i> , $\Delta lacZ4787$, <i>hsdR514</i> , Δ (<i>araBAD</i>)567, Δ (<i>rhaBAD</i>)568, <i>rph-1</i> , Δfnr	This work
Plasmids		
pK19mobsacB	Km ^R ; 5.721 kb suicide vector, <i>oriV_{Ec}</i> , <i>oriT</i> , <i>sacB</i>	(67)
pK19mobsacB- <i>goxR</i>	Km ^R ; 6.656 kb pK19mobsacB derivative containing 0.935 kb PCR fragment comprising the fused flanking regions of <i>goxR</i>	This work
pKOS6b	Km ^R , fluorocytosine-sensitive, suicide vector, derivative from pAJ63a, <i>upp</i> removed, <i>codBA</i> integrated	(68)
pKOS6b- <i>goxR-strep</i>	Km ^R , fluorocytosine-sensitive, plasmid for tagging <i>goxR</i> (GOX0974) genomically with a C-terminal Strep-tag	This work

pET-TEV	Km ^R ; pET28b derivative for overexpression of genes in <i>E. coli</i> , adding an N-terminal decahistidine tag and a TEV protease cleavage site to the target protein (pBR322 <i>oriV_{Ec}</i> , pT7, <i>lacI</i>)	(77)
pET-TEV- <i>goxR</i>	Km ^R ; 6.043 kb pET-TEV derivative encoding GoxR with an N-terminal decahistidine tag followed by a TEV protease cleavage site	This work
pMal-c	Ap ^R ; 6.148 kb P _{<i>tac</i>} -based expression vector for fusion proteins with the <i>E. coli</i> maltose-binding protein (MBP) without signal peptide;	New England Biolabs
pMal-c- <i>goxR</i>	Ap ^R ; 6.871 kb pMal-c derivative encoding a MBP-GoxR fusion protein separated by a TEV cleavage site	This work
pCP20	Ap ^R ; Cm ^R ; 9.400 kb plasmid with a temperature-sensitive replication encoding the yeast Flp recombinase	(66) CGSC, Yale, USA
pBBR-K-Pppp3-lacZ (= pLacZ)	Km ^R ; 7.416 kb pBBR1-MCS2 derivative for use as promoter probe vector with <i>lacZ</i> as reporter gene, designated as pLacZ in this study	DSM, Kaiser-augst, Switzerland
pLacZ- <i>pntA1</i>	Km ^R ; 7.629 kb pLacZ_pPPP3 derivative carrying the <i>pntA1</i> (GOX0310) promoter region (314 bp) fused to <i>lacZ</i>	This work
pLacZ_GOX0090	Km ^R ; 7.648 kb pLacZ_pPPP3 derivative carrying the GOX0090 promoter region (333 bp) fused to <i>lacZ</i>	This work
pLacZ- <i>cioA</i>	Km ^R ; 7.655 kb pLacZ_pPPP3 derivative carrying the <i>cioA</i> (GOX0278) promoter region (340 bp) fused to <i>lacZ</i>	This work
pLacZ_control	Km ^R ; 7.315 kb pLacZ_pPPP3 derivative without a promoter region in front of <i>lacZ</i>	This work
pTRc99a	Ap ^R ; <i>lacI^q</i> ; 4.176 kb expression vector with P _{<i>tac</i>} promoter and pUC18 EcoRI-HindIII polylinker region	(78)
pTRc99a- <i>goxR</i>	Ap ^R ; <i>lacI^q</i> ; 4.897 kb pTRc99a derivative for P _{<i>tac</i>} -based <i>goxR</i> expression	This work

pTRc99a- <i>goxR</i> _C14A	Ap ^R ; <i>lacI</i> ^q ; 4.897 kb pTRc99a- <i>goxR</i> derivative with a GoxR-C14A exchange (TGC→GCC)	This work
pTRc99a- <i>goxR</i> _C17A	Ap ^R ; <i>lacI</i> ^q ; 4.897 kb pTRc99a- <i>goxR</i> derivative with a GoxR-C17A exchange (TGC→GCC)	This work
pTRc99a- <i>goxR</i> _C25A	Ap ^R ; <i>lacI</i> ^q ; 4.897 kb pTRc99a- <i>goxR</i> derivative with a GoxR-C25A exchange (TGC→GCC)	This work
pTRc99a- <i>goxR</i> _C31A	Ap ^R ; <i>lacI</i> ^q ; 4.897 kb pTRc99a- <i>goxR</i> derivative with a GoxR-C31A exchange (TGC→GCC)	This work
pTRc99a- <i>goxR</i> _C113A	Ap ^R ; <i>lacI</i> ^q ; 4.897 kb pTRc99a- <i>goxR</i> derivative with a GoxR-C113A exchange (TGC→GCC)	This work

TABLE 3 Oligonucleotides used in this work

Oligonucleotide	Description or oligonucleotide sequence (5'→3') ^{a, b}	Application
0974_f1_xba_fw	GCTCTAGATGCTGTCACGGTCTTCCGGC	<i>goxR</i> deletion
0974_f1_fus_rev	<u>CATGCCTTCGGCGATCATGATGAACCCCGTTCCGT</u> TGCCTGACCTCGG	<i>goxR</i> deletion
0974_f2_pst_rev	TGCACTGCAGGATTGTTAACGCGGTCACGC	<i>goxR</i> deletion
0974_f2_fus_fw	<u>ACGGGGTTCATCATGATCGCCGAAGGCATGGAATA</u> GCCCCGCTGTTTCGCAG	<i>goxR</i> deletion
0974_region_fw	CTCTGTCAGGACAGACGTCCCG	Region primer
0974_region_rev	GCCTTCAGGAGTCTCTGAACTCCC	Region primer
0974_gene_fw	CTGCAACAGCATTGACGACTGCG	Gene primer
0974_gene_rev	AGGTAATCCGCAATGTCGGTGC	Gene primer
<i>goxR-strep_01_fw</i>	ACAGCTATGACATGATTACGGCCGGCCACGATTT CTTTG	Construction of pKOS6b- <i>goxR-strep</i>
<i>goxR-strep_02_rev</i>	CTCGAACTGTGGGTGGGACCATTCCATGCCTTCGG CGATCG	Construction of pKOS6b- <i>goxR-strep</i>
<i>goxR-strep_03_fw</i>	TGGTCCCACCCACAGTTCGAGAAGTAGCCCGCTG TTCGCAGGG	Construction of pKOS6b- <i>goxR-strep</i>
<i>goxR-strep_04_rev</i>	TGCATGCCTGCAGGTCGACTTAACGTCACCGCGG GTCTTG	Construction of pKOS6b- <i>goxR-strep</i>
pKOS6b_seq_for	TGCTTCCGGCTCGTATGTTG	Sequencing
pKOS6b_seq_rev	GGATGTGCTGCAAGGCGATTAAG	Sequencing
<i>goxR-strep_seq_fw</i>	AACAGTCAGCCGGATCCTCAG	Sequencing
<i>goxR-strep_seq_rev</i>	CTTCCTGGGACTGCTTCTG	Sequencing
0974_ex_ndeI_fw	CCCCATATGTCAGCGTCACATAGTCC	pET cloning pTrc99a cloning
0974_ex_stopxho_rev	GGGCTCGAGCTATTCCATGCCTTCGGCG	pET cloning

TEV-site- <i>Eco</i> -fw	GCGC <u>GAATTC</u> GAGAACCTGTATTTTCAGGGCCATAT G	pMalc cloning
0974_ex_stopxba_rev	GGGTCTAGACTATTCCATGCCTTCGGCG	pMalc cloning pTrc99a cloning
0090_lacZ_ <i>Eco</i> RI_fw	CG <u>GAATTC</u> ACCCTGAAGCAGGACGGAGTTACG	pLacZ cloning
0090_lacZ_ <i>Nde</i> I_rev	GGAATTC <u>CATATG</u> GGGGCGTTCTCCTGCTGGACTC	pLacZ cloning
0278_lacZ_ <i>Eco</i> RI_fw	CG <u>GAATTC</u> CATCCCGACCATGAAAGAGCG	pLacZ cloning
0278_lacZ_ <i>Nde</i> I_rev	GGAATTC <u>CATATG</u> GTCGATTGCCTTCTGGGTAGATG G	pLacZ cloning
0310_lacZ_ <i>Eco</i> RI_fw	CG <u>GAATTC</u> AAAGAAGGTCCACGAGCGC	pLacZ cloning
0310_lacZ_ <i>Nde</i> I_rev	GGAATTCATATGCTGCGATCCTGTGTCTG	pLacZ cloning
0310_Race_sp1	AGGACGATGTCGGCATCGGC	5'-RACE
0310_Race_sp2	GCTGTCGGGGTAGGACGATGC	5'-RACE
0278_Race_sp1	ATGACGAGGCCGGAGACCACGC	5'-RACE
0278_Race_sp2	AAGGTCGAGATAGGCGCTGC	5'-RACE
delta0974_seq	CATCATGTCAGCGTCACATAGTCC	Sequencing
TG40GC_fw	GATGTCCATGATCGAGCCGCCATTGCGTGGG	Mutagenesis
TG40GC_rev	CCCACGCAATGGGCGGCTCGATCATGGACATC	Mutagenesis
TG49GC_fw	GATCGATGCGCCCATGCCGTGGGCCGTCGTCTG	Mutagenesis
TG49GC_rev	CAGACGACGGCCACGGCATGGGCGCATCGATC	Mutagenesis
TG73GC_fw	CCGTCGTCTGAGTATCGCCAACAGCATTGACGAC	Mutagenesis
TG73GC_rev	GTCGTCAATGCTGTTGGCGATACTCAGACGACGG	Mutagenesis
TG91GC_fw	GCAACAGCATTGACGACGCCGATCTGGCCGTTCTTG	Mutagenesis
TG91GC_rev	CAAGAACGGCCAGATCGGCGTCGTCAATGCTGTTGC	Mutagenesis
TG337GC_fw	GCAGCGCTACGCTGGCCCGCTTTCCCATG	Mutagenesis
TG337GC_rev	CATGGGGAAAGCGGGCCAGCGTAGCGCTGC	Mutagenesis

^aUnderlined sequences denote restriction sites, double-underlined sequences denote complementary sequences. ^bOverlaps for Gibson assembly are written in bold letters.

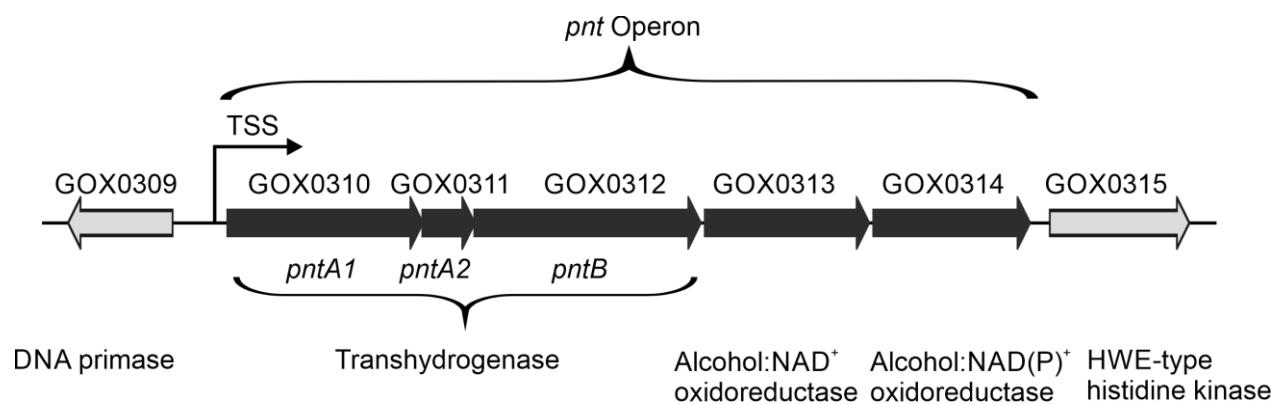


FIG 1 Chromosomal organization of the *pnt* operon, a major target of the FNR-type regulator GoxR of *G. oxydans*. Dark grey arrows mark genes regulated by GoxR, light grey arrows show neighbouring genes not regulated by GoxR. TSS, transcriptional start site.

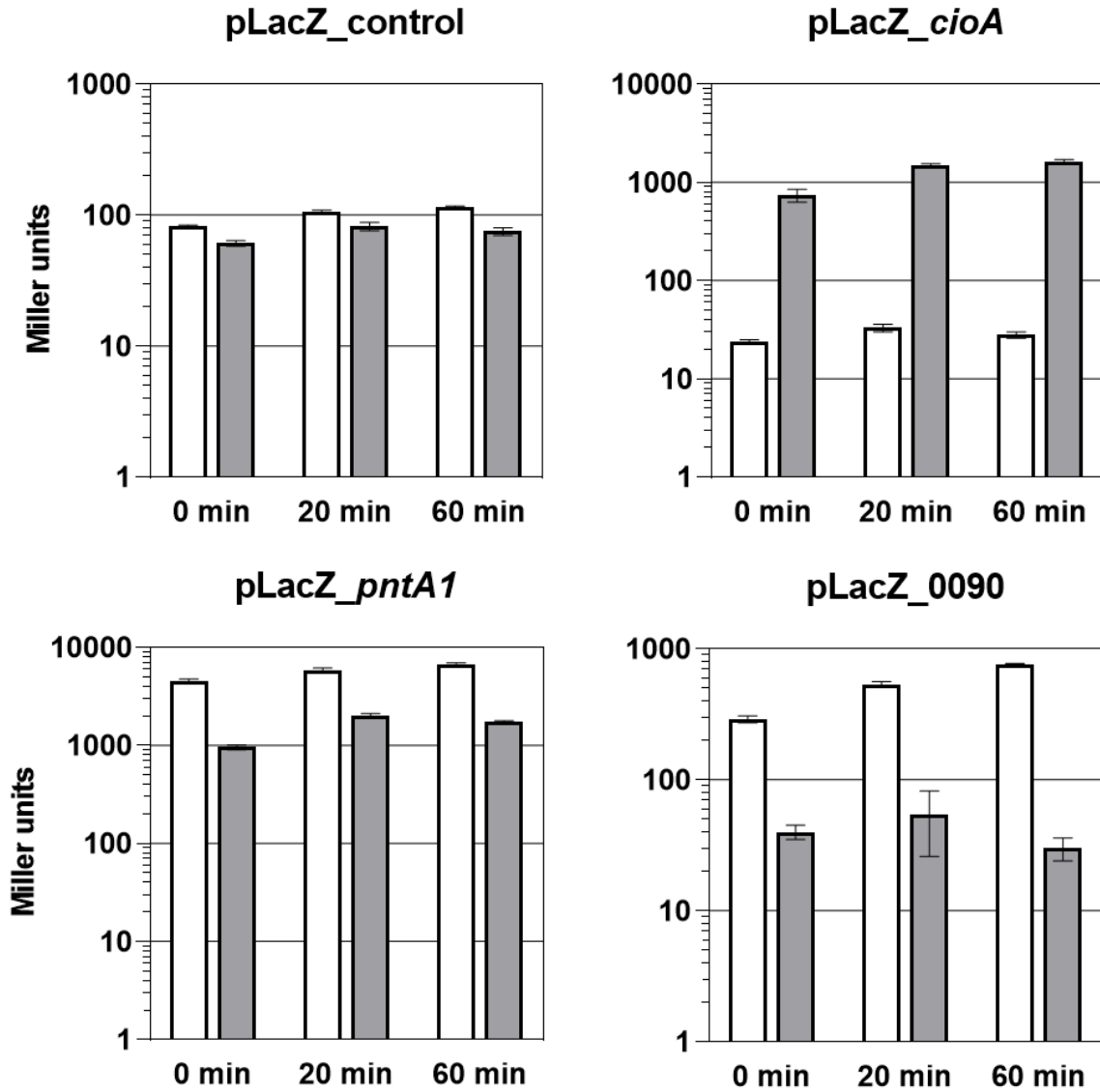


FIG 2 Analysis of the promoter activities of *cioA*, *pntA1* and GOX0090 in dependence of oxygen and GoxR using transcriptional *lacZ* fusions. The β -galactosidase activity of the parent strain (white) and the $\Delta goxR$ mutant (grey) carrying the reporter plasmids pLacZ_control, pLacZ_cioA, pLacZ_pntA1, or pLacZ_GOX0090 was measured. The strains were cultivated in a bioreactor at 15% DO to an OD₆₀₀ of 2.5 before the gassing was changed to 2% O₂/98% N₂. Samples were taken

before switching to oxygen limitation and 20 min and 60 min after the switch. Mean values and standard deviations of three biological replicates are shown.

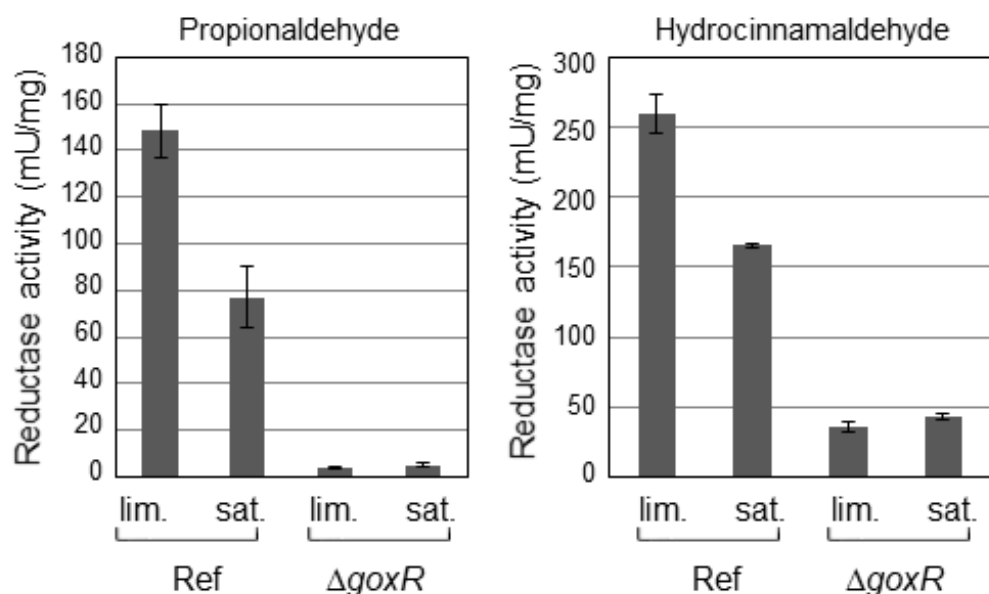


FIG 3 NADH-dependent aldehyde reductase activity in the soluble fraction of cell extracts of the *G. oxydans* parental strain (Ref) and the $\Delta goxR$ mutant ($\Delta goxR$). Propionaldehyde and hydrocinnamaldehyde were previously shown to be favorable substrates of the alcohol:NAD⁺ oxidoreductase GOX0313 of *G. oxydans* (34), whose expression is repressed by GoxR. The strains were cultivated in bioreactors either at 15% DO (sat.) or under oxygen limitation (lim.), achieved by gassing with 2% O₂/98% N₂ (0% DO) as described in the Materials and Methods section. Mean values and standard deviations of three technical replicates are shown.

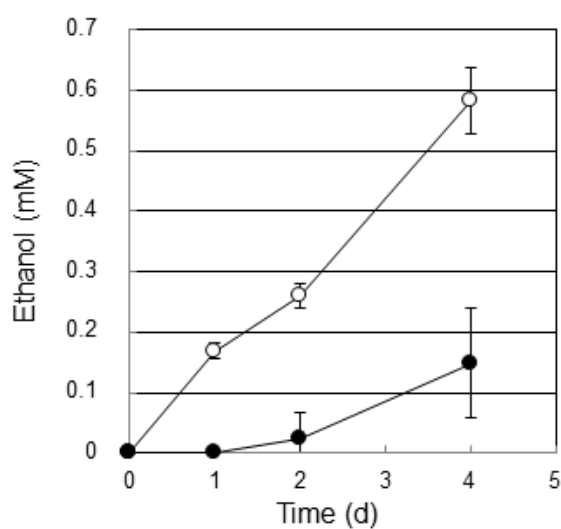


FIG 4 Ethanol production under oxygen-deprived conditions by the *G. oxydans* parent strain (open circle) and the $\Delta goxR$ mutant (closed circle). The two strains were cultivated in mannitol medium in shake flasks with vigorous shaking to the stationary phase of growth. The cells were washed, resuspended to an OD₆₀₀ of 0.5 in MES buffer (pH 6.0), and incubated under oxygen-deprived conditions in the presence of 0.4% (w/v) glucose. Mean values and standard deviations from at least four parallel experiments are shown.

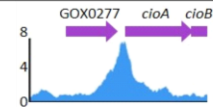
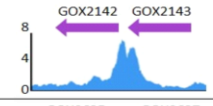
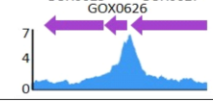
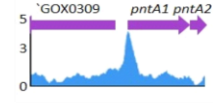
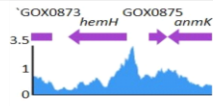
ChAP-Seq peak	Peak intensity	GoxR binding motif sequence	p-value	Distance to TSS	Regulated genes	Annotation	mRNA ratio	p-value
	7.6	TTT A GagggT TCAA TTGATtttt GTC AA	2.20E-03 4.32E-05	-2.5 -56.5	<i>cioA</i> <i>cioB</i>	Terminal oxidase CioA Terminal oxidase CioB	6.60 4.66	0.001 0.009
	7.2	TTGA G atat ATCAA	4.32E-05	-41.5	GOX2142	Hypothetical protein	0.46	0.058
	7.1	TTGATgcag ATCAA	3.98E-07	+37.5	<i>trxA</i>	Thioredoxin	3.06	0.103
	4.3	TTGATatcc ATCAA	1.00E-06	-41.5	<i>pntA1</i> <i>pntA2</i> <i>pntB</i> GOX0313 GOX0314	Transhydrogenase, α 1 Transhydrogenase, α 2 Transhydrogenase, β Alcohol:NAD ⁺ oxidored. Put. alcohol:NAD(P) ⁺ oxidoreductase	0.11 0.11 0.19 0.15 0.36	<0.001 0.003 0.010 <0.001 0.060
	3.4	ATT T Ccctt ATCAA TTGATaagg AGA AT	3.53E--03 3.53E-03	+94.5 No TSS	<i>hemH</i> GOX0875	Ferrochelatase attachment protein	2.21 1.20	0.222 0.746
	3.3	TGG T Tcggag TCTA	6.29E-03	+13.5	GOX1500 GOX1501	Put. antitoxin with YefM-like domain Put. toxin with a PIN domain acting as nuclease	2.28 2.04	0.178 0.222
	2.8	TTGATcctc GTC AT ATGACgagg ATCAA	1.89E-04 1.89E-04	-41.5 +144	GOX0090 GOX0091	ADP-dependent (S)-NADPH-hydrate dehydratase/NADPH-hydrate epimerase hypothetical protein	0.40 0.74	0.050 0.460

FIG 5 Overview on GoxR binding sites in the genome of *G. oxydans* identified by ChAP-Seq analysis that are correlated with an increased or decreased expression of the target genes. A peak intensity ≥ 2.8 was used as cut-off. From left to right, a plot of the relevant ChAP-Seq peak, the peak intensity, the GoxR binding motif sequence, the p-value of this binding motif determined with the FIMO program using the consensus sequence (TTGATnnnnATCAA), the distance of the centre of this motif to the TSS of the downstream gene, the genes regulated by this GoxR binding site, and the annotation of the corresponding genes is shown. Furthermore, the mRNA ratios (Δ *goxR* vs. parental strain) of the corresponding genes determined by RNA-Seq, and the p-values of the mRNA ratios are depicted.

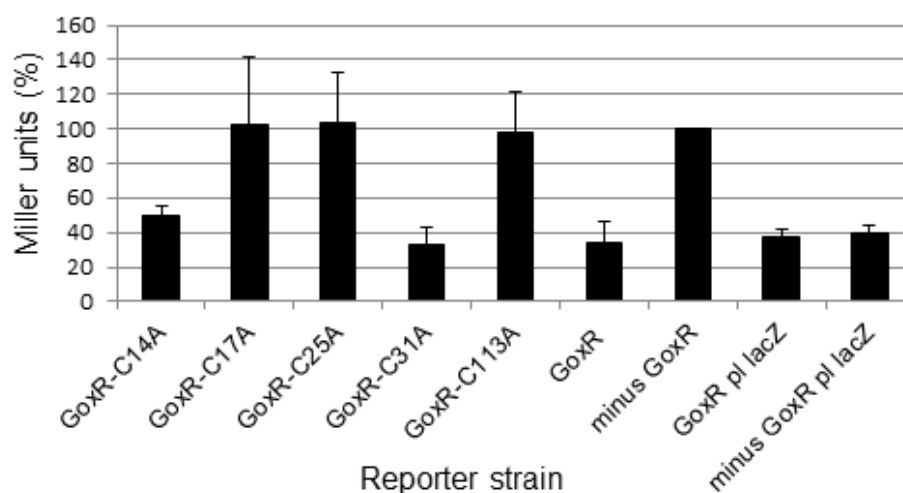


FIG 6 β -galactosidase activity of *E. coli* Δfnr strain transformed with the indicated pTrc99-based GoxR expression plasmids or the vector alone (minus GoxR) and the reporter plasmid pLacZ_*cioA* carrying the *lacZ* gene under control of the *cioA* promoter or pLacZ_control carrying a promoter-less *lacZ* gene (pl lacZ). The strains were cultivated under anaerobic conditions as described in Materials and Methods. Mean values and standard deviations of three independent biological replicates are shown.

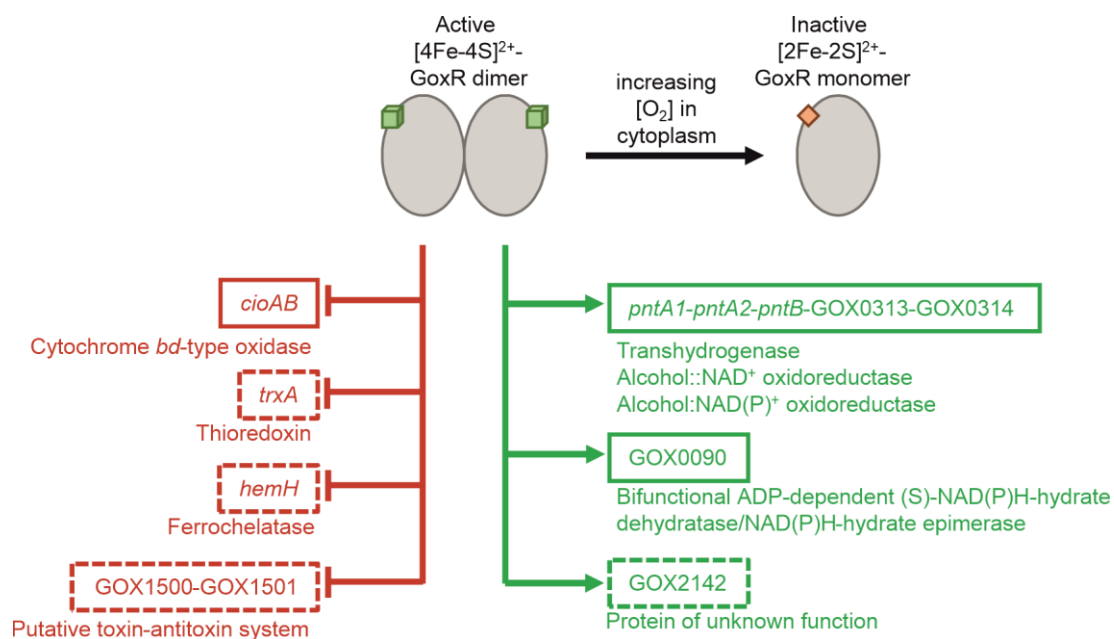


FIG 7 Model of the GoxR regulon in *G. oxydans* identified in this study. Genes that are activated by GoxR are shown in green boxes, genes that are repressed by GoxR in red boxes. For the genes in dashed boxes, the p-values for the $\Delta goxR$ /WT mRNA ratio were above the standard threshold of 0.05.

Supplementary data

The FNR-type regulator GoxR of the obligatory aerobic acetic acid bacterium *Gluconobacter oxydans* affects expression of genes involved in respiration and redox metabolism

Stefanie Schweikert^{a*#}, Angela Kranz^{a#}, Toshiharu Yakushi^b, Andrei Filipchyk^a, Tino Polen^a,
Helga Etterich^a, Stephanie Bringer^a, and Michael Bott^{#a}

^aIBG-1: Biotechnology, Institute of Bio- and Geosciences, Forschungszentrum Jülich,
D-52425 Jülich, Germany

^bDepartment of Biological Chemistry, Faculty of Agriculture, Yamaguchi University,
Yamaguchi 753-8515, Japan

TABLE S1 Overview of the 43 GoxR binding sites identified by ChAP-Seq analysis in the genome of *G. oxydans*, ordered according to their peak intensity. From left to right, the peak number, the peak intensity, the location of the peak (chromosome or plasmid), the start position and the end position of the peak, the position of the highest coverage (Pos Top Cov), the associated genes (gene ID, gene name, and annotation), the GoxR binding motif sequence, and the p-value of this binding motif determined with the FIMO program using the consensus sequence (TTGATnnnnATCC) are shown. Furthermore, the mRNA ratios (Δ goxR vs. parental strain) of the corresponding genes determined by RNA-Seq, and the p-values of the mRNA ratios are depicted. n.d.: not determined.

Peak No	Peak intensity	Chromosome/Plasmid	Start	End	Pos Top Cov	Gene ID	Gene name	Annotation
1	13.41	NC_006675_pGOX4	5769	6171	5965	GOX2720		transposase
						GOX2721		transposase
2	7.64	NC_006677_chromosome	293385	293870	293654	GOX0278	<i>cioA</i>	cyanide-insensitive cytochrome bd ubiquinol oxidase, subunit I
						GOX0279	<i>cioB</i>	cyanide-insensitive cytochrome bd ubiquinol oxidase, subunit II
3	7.22	NC_006677_chromosome	2351013	2351688	2351214	GOX2142		hypothetical protein
4	7.05	NC_006677_chromosome	667664	668119	667899	GOX0626	<i>trxA</i>	thioredoxin
5	6.15	NC_006677_chromosome	2176891	2177320	2177099	GOX1988		pyridoxine/pyridoxamine 5'-phosphate oxidase
6	5.39	NC_006677_chromosome	1174239	1174786	1174552	GOX1070		transcription termination factor Rho
7	4.29	NC_006677_chromosome	328161	328546	328363	GOX0310	<i>pntA1</i>	Transhydrogenase, subunit α 1
						GOX0311	<i>pntA2</i>	Transhydrogenase, subunit α 2
						GOX0312	<i>pntB</i>	Transhydrogenase, subunit β
						GOX0313		Alcohol:NAD ⁺ oxidoreductase
						GOX0314		Probable alcohol:NAD(P) ⁺ oxidoreductase
8	3.99	NC_006677_chromosome	751332	751854	751572	GOX0691		hemolysin D
						GOX0692		TetR-family transcriptional regulator
9	3.35	NC_006677_chromosome	943152	943594	943401	GOX0874	<i>hemH</i>	ferrochelatase
						GOX0875		bacterial archaeo-eukaryotic release factor family 12
10	3.31	NC_006677_chromosome	1644435	1644837	1644577	GOX1500		putative antitoxin with YefM-like domain
						GOX1501		putative toxin with a PIN domain acting as nuclease
11	2.84	NC_006677_chromosome	893094	893585	893366	in GOX0824		translation initiation factor IF-3

12	2.80	NC_006677_chromosome	107121	107543	107338	GOX0090	bifunctional ADP-dependent (S)-NAD(P)H-hydrate dehydratase/NAD(P)H-hydrate epimerase
						GOX0091	membrane protein
13	2.76	NC_006677_chromosome	1075884	1076289	1076015	GOX0978	bifunctional riboflavin biosynthesis protein RibD
14	2.63	NC_006677_chromosome	368405	368844	368633	GOX0347	general stress protein
						GOX0348	HlyD family secretion protein
15	2.55	NC_006672_pGOX1	20995	21431	21202	in GOX2523	DNA helicase II
16	2.55	NC_006677_chromosome	1214993	1215395	1215184	GOX1107	O-antigen biosynthesis protein
17	2.50	NC_006677_chromosome	528340	528805	528545	GOX0506	sigma factor 32 of RNA polymerase
18	2.50	NC_006677_chromosome	1567132	1567574	1567297	convergent (GOX1432 & GOX1433)	
19	2.38	NC_006677_chromosome	752872	753328	753104	in GOX0693	hypothetical protein
20	2.38	NC_006677_chromosome	1188365	1188804	1188605	GOX0182	hypothetical protein
21	2.33	NC_006677_chromosome	1229742	1230149	1228908	in GOX1122	
22	2.29	NC_006677_chromosome	1599268	1599794	1599558	GOX1461	peptidase S9
						GOX1462	aldo/keto reductase
23	2.25	NC_006677_chromosome	946364	946912	946613	GOX0877	N-acetylmuramic acid 6-phosphate etherase
24	2.21	NC_006677_chromosome	1351201	1351659	1351394	GOX1242	methylthioribulose 1-phosphate dehydratase
25	2.21	NC_006677_chromosome	1662018	1662397	1662259	GOX1508	hypothetical protein
26	2.16	NC_006677_chromosome	198806	199165	198991	GOX0182	hypothetical protein
27	2.16	NC_006677_chromosome	698491	698882	698672	GOX0648	LysR-family transcriptional regulator
						GOX0649	D-galactose transporter
28	2.16	NC_006677_chromosome	910413	910831	910622	GOX0844	DNA polymerase IV
29	2.12	NC_006677_chromosome	659781	660211	659994	GOX0616	hypothetical protein
						GOX0617	hopanoid biosynthesis associated radical SAM protein HpnH
30	2.12	NC_006677_chromosome	1084027	1084391	1084206	GOX0986	coenzyme PQQ synthesis protein B
31	2.12	NC_006677_chromosome	1372793	1373181	1372984	GOX1258	hypothetical protein
						GOX1259	hypothetical protein

32	2.12	NC_006677_chromosome	1410569	1410960	1410768	GOX1286		cell envelope biogenesis protein TonB
33	2.08	NC_006673_pGOX2	8105	8505	8307	GOX2676		glutathione-dependent formaldehyde dehydrogenase
34	2.08	NC_006677_chromosome	448658	449078	448934	GOX0423		flagellar motor switch protein FliG
35	2.08	NC_006677_chromosome	1559125	1559505	1559326	GOX1427	<i>thyX</i>	FAD-dependent thymidylate synthase
36	2.04	NC_006677_chromosome	1042894	1043380	1043099	in GOX0951		
37	2.00	NC_006677_chromosome	452676	453095	452873	convergent (GOX0426 &GOX0427)		
38	2.00	NC_006677_chromosome	1829567	1829927	1829736	convergent (GOX1672 &GOX1673)		
39	2.00	NC_006677_chromosome	2256834	2257298	2257062	GOX2060		hypothetical protein
						GOX2061		alanine racemase
40	1.95	NC_006677_chromosome	1071120	1071525	1071332	convergent (GOX0972 &GOX0973)		
41	1.95	NC_006677_chromosome	2049734	2050110	2049919	GOX1870		hypothetical protein
						GOX1871		hypothetical protein
42	1.87	NC_006677_chromosome	768522	768886	768684	GOX0706		phosphate ABC transporter permease
						GOX0707		DNA starvation/stationary phase protection protein
43	1.78	NC_006677_chromosome	1228742	1229129	1228908	GOX1122		putative NAD-dependent aldehyde dehydrogenase

Go-GoxR	-----MSASHSPEDVHDRCAHCVGRRLSICNSIDDCDLAVLANESSR-M	43
Aa-' GoxR'	-MSVSALTAGNSLSVPKRIVIAGMEGCRACSVCEVRAHGICCSALNDDLSQLAQAAVR-V	58
Gd-' GoxR'	--MSDQTT CERESRPRLILAGAHQPGYCLTCGVRPRSVCSAISDDDIVRLAETAVE-T	57
Ks-' GoxR'	--MSDMPSCQFESRPRRIMMGPSGLQTDFCATCTVRPNSVCNVIDEGLSRLAEAAVE-T	57
Kb-' GoxR'	-----MRTNDTVRAIGHCGQCEQCEHCARSQSICSVIDQRDHLQALHLSQR-I	48
Ab-' GoxR'	-----MDAQTRDSISALGPCGSCGQCCLHCEARTRSICSVIDPDNMARLAQYSHR-L	50
Bj-FixK1	-----MKPSVVMIEPNGHFCSDCAIRTSAVCSSLDAAELREFEHLGRR-V	44
Rl-FnrN	-----MDVAHSGVLEVGIPVACRSCQARHGVCVGLSSGQLKDLGRHSLR-R	46
Av-CydR	-----MSDKSKVRPVHHIRCQECSLAALCLPISLNFEDIDALNEIVKRGK	45
Af-FNR	-----MMSDNSANKRIQSGGCAIHCQDCSISQLCIPFTLNDSQLDEIERKK	50
Ec-FNR	-----MIPEKRIIRRIQSGGCAIHCQDCSISQLCIPFTLNEHQLDNIERKK	50
	* * : : . : .	
Go-GoxR	TVADGRSFIEEGAPAHDFVVTGGRVKLFLLPDGRRQITGFAEGGDFLGLAAS--TSYA	101
Aa-' GoxR'	TIPPGRQLIEEGSPADEFNITAGTVKLFKSLPDGRRQITGFVGIGHFLGLAVS--DRYA	116
Gd-' GoxR'	LVLPGRAFVEEGAPATDFFSITSGNVKLFKALPDGRRQITGFAGAGHFLGLAVT--DQYA	115
Ks-' GoxR'	IIPPGRGFIEEGAPATDFFNVTAGTVKLFKALPDGRRQITGFAAPGHFLGLAVS--DSYA	115
Kb-' GoxR'	EIPSGRCFIEEGETARDFIVTDGHAKLFNLLPDGRRQITGFADCGQFLGLASI--ENYA	106
Ab-' GoxR'	SVAPGKTFIQEGEAATDFYIVTAGHVKIFTLMPDGRRQITGFGQSGDFLGLASG--ATYA	108
Bj-FixK1	HFSSGETVFSEEDITTSFYNVLEGMRLYKLLPDGRRQIVGFALPGDFLGMNLS--GRHN	102
Rl-FnrN	KVDAGCEIIAQGSESSFYSNIMSGVVKLCKVMPDGRHEIVGLQFAPDFVGRPFV--REST	104
Av-CydR	PIKKGEFLFRQGDAGFSVFAVRSGSLKTFVSVDNGEEQITGFHLPSSELVGLSGMDSDCP	105
Af-FNR	PIQKGQELFKAGDELKCLYAIRSGTIKSYTITEQGDEQITAFHLAGDLVGFDIAEAQHP	110
Ec-FNR	PIQKGQTLFKAGDELKSLYAIRSGTIKSYTITEQGDEQITGFHLAGDLVGFDIAISGHHF	110
	. * .. : * : . : * : * : . : *	
Go-GoxR	FGAEALGSATLCRFPHAGMQRLTERFPSLEHRLREEASRELALMQARMTLLGRKTARERV	161
Aa-' GoxR'	FGAEAIDQVRLCRFSRERLETVIDEFPRLERLRNEAANELVAAQDQMLLLGRKTARERV	176
Gd-' GoxR'	FGAEAVDTVRLCRFSRARMRHLMDDFPRLERRLLEEASNELVAAQNQMLLLGRKTARERV	175
Ks-' GoxR'	FGAEAIDTVRVCRFSREKMTLDDDFPKLERRLLEEASNELVAAQNQMLLLGRKTARERV	175
Kb-' GoxR'	FSAEALTPLRVCRFSHIGMSLLKTQFPALERRLLEEASSELVRAQARMLLLGRKTARERL	166
Ab-' GoxR'	FSAEALGPLSLCRFSRTGLGLLRREFPALELRLMEEASRELVQAQRMLLLGRKTARERL	168
Bj-FixK1	FSADAIGAVTVCFQAKAPFGRFIEERPQLLRRINELAIRESQARDHVMVLLGRRSADKVV	162
Rl-FnrN	LSAEAAATDAEICVFPRLSLDRMISPELQSLHDQALKELDAAREWIVTLGRRTAEKVV	164
Av-CydR	VSAQALETTSVCEIPFERLDELALQLPQLRRQLMRVMSREIRDDQMMMLLSKKTADERI	165
Af-FNR	SFAQALETSMVCEIPYEILDDLSGKMPKLRQQIMRLMSNEIKGDQEMILLSSKKNAEERL	170
Ec-FNR	SFAQALETSMVCEIPFETLDDLSGKMPNLRQQMMRLMSGEIKGDQDMILLSSKKNAEERL	170
	* : * : : . * * : * : : * : * : *	
Go-GoxR	ATFLIERCTHLDRP-DSARPVELDLPMPRTDIADYLGLTIETVSRLSAFKKEKLISIRS	220
Aa-' GoxR'	ASFLYGQITELYGD-DIPQTAKLHFPMTADIADFLGLTVETVSRTISGLRREGLITIGA	235
Gd-' GoxR'	ASFLLDVRDMLNPSPG-----DVPLPMTRSDIADYLGLTIETVSRTLSSWMRTERLITIGK	230
Ks-' GoxR'	ASFLLDQMRIGQPPAGNGGPCRLNLPMTGRDIADYLGLTIETVSRTLSSWMRSQGMIEVKG	235
Kb-' GoxR'	ASFLLERQEVAPR-----SD-VLILPMTRTDIADYLGLTIETVSRTLNAFRDKLIEIDH	220
Ab-' GoxR'	ASFLLEQHRSPT-----KEIVIHLPMSRTGIADYLGLTIETVSRTLNALQREMMITITQ	223
Bj-FixK1	AAFLLGWRERLLALKG--ASDTVPLPMSRQDIADYLGLTIETVSRTFTKLERHGAIAIIH	220
Rl-FnrN	ASLLHLIATHAEPQ--TATSTAFDPLSRAEIADFLGLTIETVSRLQMTLRKSGVIRIEN	222
Av-CydR	ATFLINLSSRFRR--GFSANHFRLAMSRNEIGNYLGLAVETVSRVFSRFQONELIAAE-	222
Af-FNR	AAFLYNLSTRFHQR--GFSPREFRLTMTRGDIGNYLGLTVETISRLLRGRFQKTEMLTVK-	227
Ec-FNR	AAFIYNLSRRFAQR--GFSPREFRLTMTRGDIGNYLGLTVETISRLLRGRFQKSGMLAVK-	227
	* : : . : * * : * : * : * : *	
Go-GoxR	ITHITLLMPERISTIAEGME---	240
Aa-' GoxR'	SHEITVPAPSLRTIASGEE---	255
Gd-' GoxR'	GHTVRITAMERLES LASGNS---	250
Ks-' GoxR'	GYAITLLSVSRDLVLASGNG---	255
Kb-' GoxR'	ITSIKLLNLTEIRLLADGEGF--	241
Ab-' GoxR'	VTQITLLNLPALHLARGG----	242
Bj-FixK1	G-GISLLDPARVEALAAA-----	237
Rl-FnrN	FRHIIVPDMDELERMISA-----	240
Av-CydR	GKEVTILNPVELCSLAGNMEA-	244
Af-FNR	GKYITINDHDALAE LAGSAKEIK	250
Ec-FNR	GKYITIENNDALAQ LASHTRNVA	250
	: : : :	

FIG S1 Multiple sequence alignment of GoxR from *G. oxydans* with other members of the FNR family of transcriptional regulators. The proteins labeled ‘GoxR’ represent homologs from species belonging to different genera of the family Acetobacteraceae: Aa, *Acetobacter aceti* (WP_010668045.1); Gd, *Gluconacetobacter diazotrophicus* (WP_012224455.1); Ks, *Kozakia baliensis* (WP_029603626.1); Kb, *Komagataeibacter saccharivorans* (WP_102324963.1); Ab, *Asaia bogorensis* (WP_122050810.1). The other proteins are: Bj-FixK1, *Bradyrhizobium japonicum* FixK1 (P29286.1); Rl-FnrN, *Rhizobium leguminosarum* bv. *viciae* FnrN (AAA86478.1); Av-CydR, *Azotobacter vinelandii* CydR (ACO78198.1); Af-FNR, *Aliivibrio fischeri* FNR (AAW85803.2); Ec-FNR, *Escherichia coli* FNR (WP_052931058.1). The cysteine residues demonstrated or predicted to be involved in the formation of the [4Fe-4S] cluster are shown as white letters shaded in black, another non-conserved cysteine residue present in the N-terminal part of GoxR is shaded in grey. The amino acid residues forming the DNA recognition helix are shaded in grey, too. Asterisks indicate identical amino acids, points indicate conservative substitutions.



FIG S2 Results of 5'-RACE experiments for the determination of the transcriptional start sites of *cioA* (GOX0278) and *pntA1* (GOX0301).

A. *cioA* promoter region (GOX0278)

GoxR box (-56.5) -35
CCCCGGATGCCGCA**TTGAT**TTTT**GTCAA**AATCATGTCCGGA**GTATCAA**ACTTTTCTGGCAAAA
GoxR box (-2.5)
-10 TSS*
TACGTTTAGAGGG**TCAA**AAGACGGCAACACGCGAAGAGATCACAGCTTCGTTACCCTGTTGTG
CGTGCGTGAGGCCCCCGGGAGCCGACATCCTTCCTGCCGGTCTCTGCGTTTCGCCATCTACCC
cioA coding sequence putative TSS**
AGAAGGCAATCGAC**ATG**TTTGGCTTGTCGGCTCTATTCTTGGCGC**G**TTTCCAGTTCGCGTTTAC

B. *pntA1* promoter region (GOX0310)

GoxR box (-41.5) -35 -10
ATATAATTTCTCCCTT**TTGAT**ATCC**ATCAA**TGGTTTCCACCCGAAGAAGCGT**CATGGT**GGCGC
TSS*
T**G**AACGGGGCGCGGGTTCTCTTTGCTCAGCCTGCGCTCGGCGACAGCCCGCGCCCGACGACAGA
pntA1 coding sequence
CACAGGATCGCAGCCA**ATG**ACTGTCAAGATTTCAGTCCTGAAAGAACGCGACGAAGGCGGGGAA

C. GOX0090 promoter region

GoxR box (-41.5) -35 -10
CTCCAGATGATCGACCCTGTCA**TTGAT**CCTC**GTCAT**GG**TTGAAA**ATGGAAAAAGGGG**GAAGAA**
TSS**
CATTCCC**G**AAGCATTTCCTGAATACCCGACGCAAGCCCCTCAGCGCCAGAGGGAAGCGGAATT
GAGGGACCCCGAAAGAGGCAACGCAACAGCCGGTCATGCTTTGCTGTCATGAGTCCAGCAGGAG
GOX0090 coding sequence
AACGCCCCGAG**ATG**CCAAGCCCTGAAATATCCAGCCCTGTATCCCGCCATCCTTTTCGCATTGCG

FIG S3 Promoter regions of the genes *cioA*(A), *pntA1* (B) and GOX0090 (C) with the transcriptional start sites (TSS) identified by 5'-RACE and RNAseq (*) or just by RNAseq (**), the deduced -10 and -35 regions, and likely GoxR binding sites (highlighted in green) including the distance from the center of the binding site to the TSS.

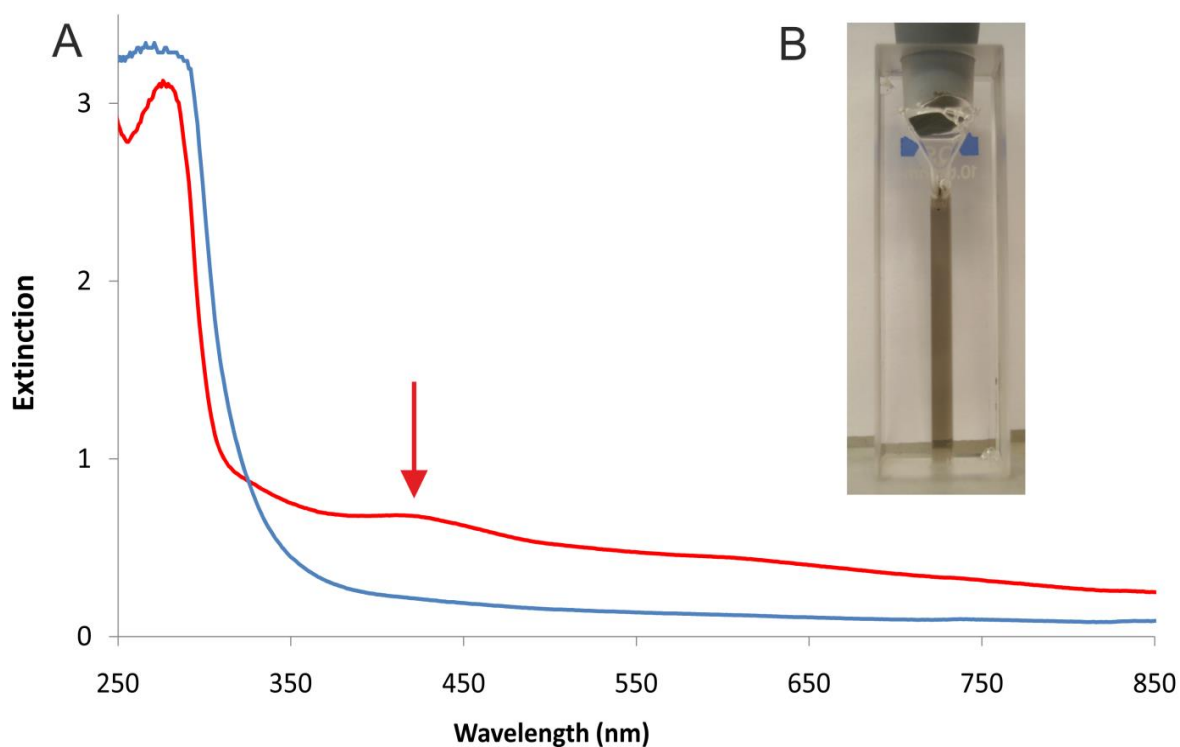


FIG S4 Evidence for the presence of an iron-sulfur cluster in the *G. oxydans* GoxR protein. A, UV/Vis spectra of elution fraction 3 obtained by amylose affinity chromatography under anoxic conditions of an MBP-GoxR fusion protein synthesized in *E. coli* BL21(DE3). The red spectrum was obtained under anaerobic conditions. The blue spectrum was obtained after incubation of the same sample for seven hours under aerobic conditions. B, Photograph of elution fraction 3 of anaerobically purified MBP-GoxR in a quartz cuvette filled in an anaerobic chamber and closed with a rubber stopper to maintain anoxic conditions. The protein solution showed a brownish to dark green color which disappeared after aerobic incubation.